Similarity of Sensitivity Functions of Reaction Kinetic Models

István Gy. Zsély, Judit Zádor, and Tamás Turányi*

Department of Physical Chemistry, Eötvös University (ELTE), H-1518 Budapest, P.O. Box 32, Hungary

Local sensitivity functions $\partial Y_i/\partial p_k$ of many chemical kinetic models exhibit three types of similarity: (i) *Local similarity*: ratio $\lambda_{ij} = (\partial Y_i/\partial p_k)/(\partial Y_j/\partial p_k)$ is the same for any parameter k. (ii) *The scaling relation*: ratio λ_{ij} is equal to $(\mathrm{d}Y_i/\mathrm{d}z)/(\mathrm{d}Y_j/\mathrm{d}z)$. (iii) *Global similarity*: ratio $(\partial Y_i/\partial p_k)/(\partial Y_i/\partial p_m)$ is constant in a range of the independent variable z. It is shown that the existence of low-dimensional slow manifolds in chemical kinetic systems may cause local similarity. The scaling relation is present if the dynamics of the system is controlled by a one-dimensional slow manifold. The rank of the local sensitivity matrix is less than or equal to the dimension of the slow manifold. Global similarity emerges if local similarity is present and the sensitivity differential equations are pseudohomogeneous. Global similarity means that the effect of the simultaneous change of several parameters can be fully compensated *for all variables, in a wide range of the independent variable* by changing a single parameter. Therefore, the presence of global similarity has far-reaching practical consequences for the "validation" of complex reaction mechanisms, for parameter estimation in chemical kinetic systems, and in the explanation of the robustness of many self-regulating systems.

1. Introduction

Sensitivity analysis is an effective tool for the exploration of the relation between the output of mathematical models and the input data, which comprise the values of parameters as well as the initial or boundary conditions. Dynamical mathematical models include chemical kinetic models, and sensitivity analysis has been widely used in reaction kinetics since the early eighties. Local sensitivities are the partial derivatives of model output with respect to the parameters and describe the effect of small parameter perturbations. There is no a priori reason sensitivity functions should be similar to each other in the case of a general mathematical model.

Reuven et al.[1] tested a new code for the calculation of local sensitivities of two point boundary value problems. The sample system was a 1D laminar flame with a symbolic reaction mechanism containing three species, a reactant, an intermediate, and a product. They found that the sensitivity−distance curves were very similar to each other for all parameters. Reuven et al. applied this code for the simulation of premixed flat hydrogen−air[2] and CO/H$_2$/O$_2$ [3] flames, and again the sensitivity functions were found to be similar. They also noticed that this similarity disappeared if temperature was not calculated, but the temperature profile was fixed to the previously calculated values. Rabitz and Smooke[4] provided an explanation of this interesting result. They stated that a strong coupling between the variables, like the calculated temperature in combustion systems, implies two types of similarity between the sensitivity functions. The first one is that the ratio of the sensitivities of two variables with respect to the same parameter is equal for any parameter and that it is also equal to the ratio of the gradients of the corresponding variables with respect to the independent variable. The second one is that the ratio of the sensitivities of any variable with respect to any two parameters is equal at any

value of the independent variable (e.g. distance in the case of stationary flames). Rabitz and Smooke[4] called these similarity features the *scaling relation* and *self-similarity*, respectively. Vajda, Rabitz, and Yetter[5] investigated several models of hydrogen−air homogeneous explosions and laminar flames to study the role of diffusion in the emergence of similarity. They reported that similarity could not be observed in purely temporal systems and concluded that diffusion was needed to render the sensitivity functions similar. Vajda and Rabitz[6] provided a deeper theoretical insight into the origin of similarities, but this derivation was valid only for the case of a single-step, homogeneous, exothermic reaction.

In this work, statements of papers[1−6] are reinvestigated and, in some cases, different conclusions are drawn. We found that the scaling relation is not related to the assumption that temperature is a dominant variable in adiabatic combustion systems and diffusion is not needed for the emergence of similarity. Instead, we claim that the existence of one-dimensional slow manifolds in chemical kinetic systems causes the scaling relation and that diffusion decreases the level of similarity.

In section 2, background information to the numerical examples is provided. In the next section, sensitivity functions are presented for models of stoichiometric hydrogen−air explosions and premixed laminar flames, and the similarity of the sensitivity functions is demonstrated by plotting the appropriate ratios of sensitivity coefficients. The preceding sections provide a framework in section 4 for the discussion of the previous results on the similarity of sensitivities. It is unusual to place the discussion of the literature after new results, but the prior inspection of the numerical results makes the brief literature review section much more understandable. In section 5, the emergence of the scaling relation is explained using the low-dimensional manifold theory. In the next section, the origin of the global similarity is discussed. In section 7, the importance

---

* Corresponding author. E-mail: turanyi@garfield.chem.elte.hu.

Similarity of Sensitivity Functions

J. Phys. Chem. A, Vol. 107, No. 13, 2003 **2217**
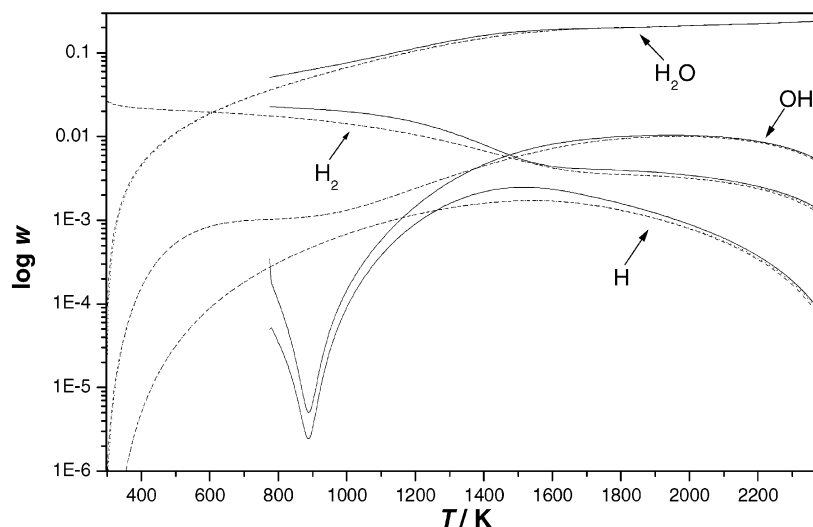
Figure 1. Mass fractions of species H, OH, H_2, and H_2O as a function of temperature for adiabatic combustion of stoichiometric hydrogen−air mixtures: (a) homogeneous explosion (solid lines); (b) freely propagating flame (dotted lines); (c) burner-stabilized flame (dashed lines). The dotted and the dashed lines almost exactly coincide. The cold boundary conditions of the flames are $p = 1$ atm and $T_c = 298.15$ K.

of the similarity of sensitivity functions is emphasized, showing its consequences on model identification and parameter estimation.

2. Background of the Numerical Examples

The numerical examples in this paper are related to the combustion of hydrogen or methane. In the methane combustion calculations, the Leeds methane oxidation mechanism[7] was used, which contained 37 species and 350 reactions. In the hydrogen combustion calculations, a submechanism of the Leeds mechanism was applied that contained the hydrogen oxidation steps only. This submechanism had 9 species and 46 reactions. Both mechanisms can be downloaded from the Web.[8]

The numerical examples were elaborated by the programs of the CHEMKIN-II package.[9] Homogeneous explosions were calculated by SENKIN,[10] and premixed laminar flames were simulated by PREMIX.[11] The freely propagating laminar premixed flames had cold boundary conditions $p = 1$ atm, $T_c = 298.15$ K, and fuel-to-air ratio $\varphi = 1.0$. At the hot boundary, the gradients of concentrations and temperature were zero; therefore, the hot boundary state was equal to the burnt equilibrium state. Since it was an adiabatic flame, the cold and hot boundary gas mixtures had to have the same enthalpy. For numerical reasons, there was a small difference in enthalpies, which could be decreased by applying more nodes in the hot region and using lower error tolerances. We wanted to compare the calculated concentrations and sensitivities of the homogeneous explosions to those of laminar flames; therefore, the initial concentrations of homogeneous explosions were determined in the following way. The enthalpy of the hot boundary mixture was set to that of the cold boundary by slightly changing temperature. The corrected hot boundary and the cold boundary compositions were mixed. The resulting mixture had the same composition of elements and the same enthalpy. The ratio of the cold gas was gradually increased, and the mixture having the lowest temperature but still able to explode within 10^{-3} s was used as the initial composition in the homogeneous explosion simulations. Figure 1 shows the concentration of some selected species as a function of temperature during homogeneous adiabatic explosion of a stoichiometric hydrogen−air mixture.

In the first series of homogeneous explosion calculations, the temperature−time curves were calculated assuming *adiabatic* conditions. This temperature−time function was recorded, and in the second series of calculations, the concentration−time curves were calculated while temperature was changed over time according to the recorded data. Such calculations were called *constrained temperature* simulations. In this case, all calculated concentrations were identical to the adiabatic explosion results. Similar constrained temperature calculations were carried out for all flame simulations; in this case, the temperature−distance functions were determined from adiabatic flame calculations. This procedure is usually not used in combustion simulations, because after much effort identical concentration profiles are obtained. However, an important feature of the sensitivity functions is that these are substantially different in the adiabatic and constrained temperature models.

For the stationary simulation of freely propagating flames, the coordinate system moves with the flame front and it is fixed to a point of a given temperature flame. For numerical reasons, this reference temperature has to be close to the cold boundary temperature and the recommended value is about 100 K above it. In our calculations, the reference temperature was always 400 K. For the case of burner-stabilized flames, the starting point of the coordinate system is the burner-surface and the shape of the flame is determined by the mass flow rate of the fuel−air mixture. At low mass flow rates the flame front is close to the burner surface and there is significant heat loss at the surface. If the mass flow rate corresponds to the velocity of the freely propagating flame, the heat loss becomes negligible, the flame becomes adiabatic, and the temperature and concentration profiles become similar to those of the freely propagating flames. Figure 1 shows the calculated mass fractions of some selected species as a function of temperature in adiabatic stoichiometric freely propagating and burner-stabilized 1D hydrogen−air flames. The concentration−temperature curves are almost identical for these two types of flames. These concentration curves are very similar to those of the adiabatic explosion above about 1300 K. In adiabatic explosion calculations enthalpy is preserved with high accuracy, unlike in the flame calculations, which cause a small deviation in the burnt states.

To facilitate the comparison of simulation results for explosions and flames, in all figures the results are plotted as a

function of temperature instead of time or distance. Since temperature continuously increases with time and distance in adiabatic homogeneous explosions and laminar flames, respectively, this is an equivalent representation of data. Such figures provide extra information, because the dominant processes in the various temperature regions of hydrogen and methane flames are known from the textbooks of combustion chemistry (see e.g. ref 12).

In the original Leeds methane oxidation mechanism,[7] for most of the reactions only the Arrhenius parameters of the forward reactions were given. During the simulations, the rates of the forward reactions were calculated from these Arrhenius parameters while the rates of the backward reactions were determined from the forward rates and the thermodynamic equilibrium values. Reactions handled this way are called here "reversible reactions". Using the program MECHMOD,[13] all reversible reactions were converted to pairs of irreversible reactions by calculating the Arrhenius parameters of the backward reactions. This "irreversible only" mechanism resulted in concentration–time curves almost identical to those of the original mechanism. The sensitivities presented in this paper are with respect to the pre-exponential factor of the reactions. All sensitivity curves were calculated for both the "reversible only" and the "irreversible only" versions of the mechanisms. The similarity relations were alike in the two series of sensitivity calculations, but the similarity of the sensitivities of the burner-stabilized flames was more clear for the "irreversible only" case; therefore, the sensitivity results for the irreversible mechanisms are presented here. Note that when perturbing the pre-exponential factor of a reversible reaction, the thermodynamic equilibrium state remains identical, since the perturbation affects the kinetic features only, and the perturbation diminishes near the equilibrium. When perturbing the pre-exponential factor of an irreversible reaction, the point of equilibrium is dislocated and therefore the sensitivity functions do not approach zero at the equilibrium.

3. Similarity of Sensitivity Functions

Changes of concentration and temperature in a constant-pressure, spatially homogeneous reaction system can be described by the following initial value problem:

$$d\mathbf{w}/dt = \mathbf{f}_w(T, \mathbf{w}, \mathbf{p}), \quad \mathbf{w}(0) = \mathbf{w}^0 \tag{1a}$$

$$dT/dt = f_T(T, \mathbf{w}, \mathbf{p}), \quad T(0) = T^0 \tag{1b}$$

where T is temperature, t is time, $\mathbf{w}$ is the N-vector of mass fractions, $\mathbf{p}$ is the M-vector of parameters, and T^0 and $\mathbf{w}^0$ are the initial values of temperature and mass fractions, respectively. The solution of the initial value problem (eq 1) means the calculation of concentration–time and temperature–time curves. Let $\mathbf{Y}$ denote the vector of variables, that is $\mathbf{Y} = (\mathbf{w}, T)$ and accordingly $\mathbf{f} = (\mathbf{f}_w, f_T)$. The parameter vector $\mathbf{p}$ includes the Arrhenius coefficients of reactions, the heat of formation of species, and so forth.

Sensitivity analysis is the name of a family of mathematical methods that studies the relationships between information flowing in and out of models.[14] Local sensitivity analysis is now widely used in chemical kinetics.[15−17] The local sensitivity coefficient $s_{ik} = \partial Y_i / \partial p_k$ gives information on the effect of the small change of the parameter p_k on model output Y_i. The sensitivity coefficients constitute the first-order local sensitivity matrix $\mathbf{S} = \{\partial Y_i / \partial p_k\}$. This sensitivity matrix can be calculated by solving the following initial value problem:

$$\dot{\mathbf{S}} = \mathbf{JS} + \mathbf{F}, \quad \mathbf{S}(0) = \mathbf{0} \tag{2}$$

where $\mathbf{J} = \partial \mathbf{f}/\partial \mathbf{Y}$ is the Jacobian and $\mathbf{F} = \partial \mathbf{f}/\partial \mathbf{p}$. Let $\mathbf{s}_i^T = \partial Y_i/\partial \mathbf{p}$ denote the vector of the ith row of the sensitivity matrix, where the superscript T denotes the transpose of a vector. In the general case, there is no functional dependence between the sensitivity coefficient–time functions. However, in many chemical kinetic simulations the calculated sensitivity functions show remarkable similarities.

Figure 2 presents the sensitivity functions of temperature and of the mass fractions of H and H_2O with respect to the pre-exponential parameters of all rate expressions for the adiabatic, homogeneous explosion of a stoichiometric hydrogen–air mixture. The sensitivity functions with respect to all parameters are strikingly similar. This similarity is more emphasized if the following ratio is derived:

$$\lambda_{ijk}(t) = \frac{s_{ik}(t)}{s_{jk}(t)} \tag{3}$$

Figure 3 shows the ratios $s_{H,k}/s_{H_2O,k}$ and $s_{OH,k}/s_{T,k}$ as a function of temperature. In this figure and in all subsequent figures that illustrate ratios of sensitivities, only the significant sensitivity functions are considered. A sensitivity function is considered significant if the absolute value of it at any temperature reaches 5% of the peak absolute sensitivity of the most sensitive parameter. The single lines between 900 and 2000 K demonstrate the exact matching of 10 lines. The sensitivity functions of the other 36 pre-exponential factors have very small values at all temperatures. The calculated values of small sensitivity elements have a large numerical error; therefore, the ratio (eq 3) for them does not agree with that of the other sensitivity pairs. Some parameters may be ineffective, and therefore, the corresponding sensitivity elements are exactly zero. These sensitivities should be excluded from the comparisons, even if the exact values of sensitivities were known.

Above about 900 K there is an autocatalytic increase of the concentration of hydrogen atom (see also Figure 1). Figure 3 indicates that in the case of the explosion of hydrogen–air mixtures, above this temperature the ratio of sensitivities for two variables is independent of the parameter perturbed. Plotting the sensitivity ratios of a "reversible only" mechanism, the lines do not deviate above 2000 K, showing that the reason for the high-temperature deviation of lines is the dislocation of the equilibrium in the irreversible case.

The property of sensitivity functions that the ratio of them is equal for any parameter will be called here *local similarity*, because the ratio λ_{ij} changes with time. Another depiction of local similarity is that at a given time any row of the sensitivity matrix can be obtained from any other row by multiplying it by a scalar:

$$\mathbf{s}_i^T(t) = \lambda_{ij}(t)\mathbf{s}_j^T(t) \tag{4}$$

Let us now consider the ratio of the gradient of variables over time:

$$\lambda'_{ij}(t) = \frac{\dfrac{dY_i}{dt}(t)}{\dfrac{dY_j}{dt}(t)} \tag{5}$$

Parts a and b of Figure 4 show the ratio λ' for the variable pairs w_H, w_{H_2O} and w_{OH}, T, respectively. The calculated λ'_{ij}– temperature curves are exactly identical to the previously calculated λ_{ij}–temperature curves in the temperature region

Similarity of Sensitivity Functions

J. Phys. Chem. A, Vol. 107, No. 13, 2003 **2219**
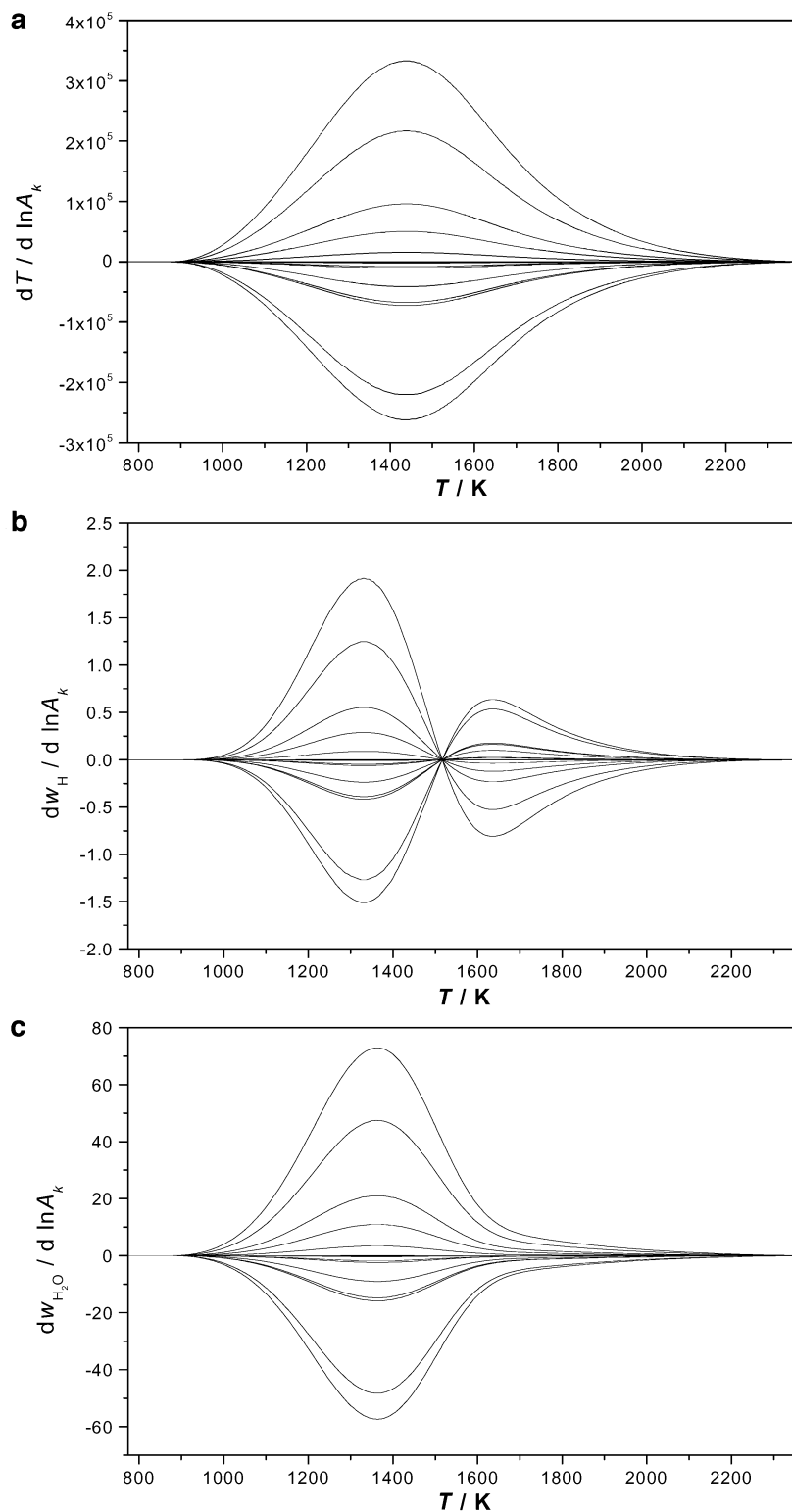
Figure 2. Sensitivities as a function of temperature calculated for the adiabatic explosion of a stoichiometric hydrogen−air mixture. Note, that seminormalized sensitivity coefficients, e.g., $dw_H/d \ln A_k = A_k(dw_H/dA_k)$, are drawn to make the sensitivities of comparable magnitude. Sensitivity coefficients belonging to (a) T, (b) H, and (c) H_2O are plotted.

900−2000 K. This identity was called the *scaling relation* of local sensitivities by Rabitz et al.[2,4] Combination of eqs 4 and 5 yields

$$\mathbf{s}_i^T(t) = \frac{\dfrac{dY_i}{dt}(t)}{\dfrac{dY_j}{dt}(t)} \mathbf{s}_j^T(t) \qquad (6)$$

Equation 6 shows that the scaling relation implies local similarity. However, we will show later that in some systems local similarity for some pairs of sensitivity coefficients may exist without the occurrence of the scaling relation.

Let us now calculate another ratio of sensitivities:

$$\mu_{ikm}(t) = \frac{s_{ik}(t)}{s_{im}(t)} \qquad (7)$$
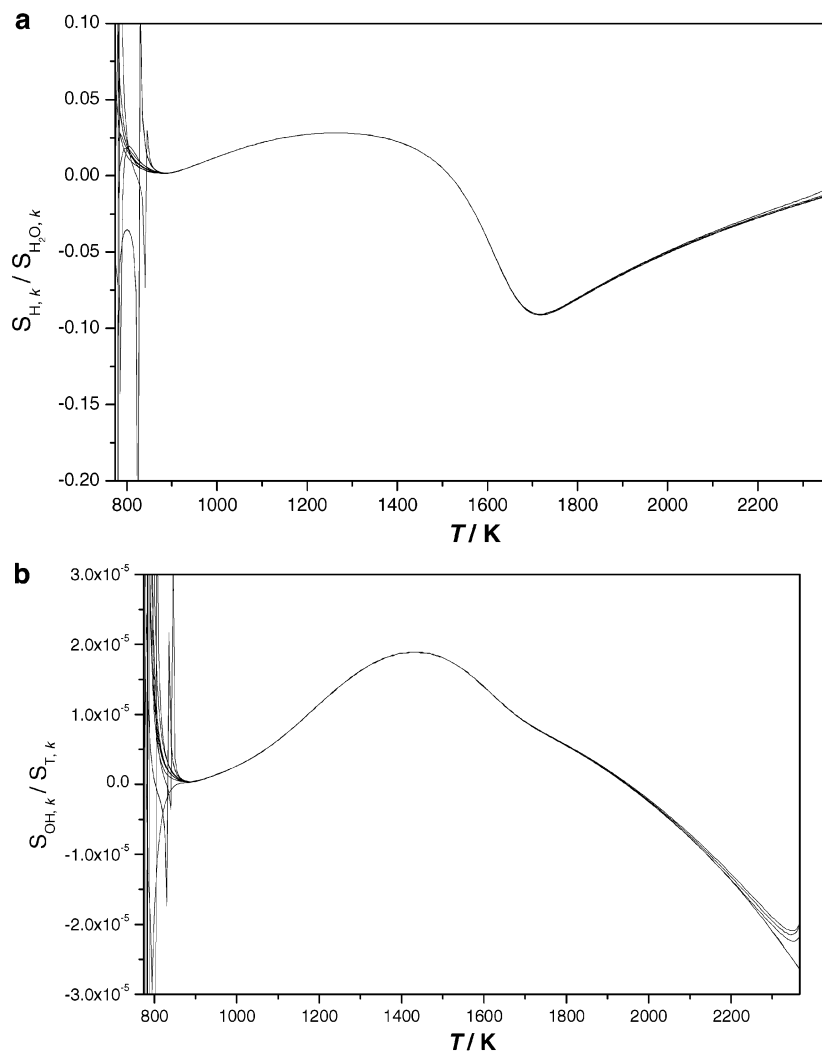
Figure 3. Ratio of sensitivity functions for two variables with respect to the same parameters for the adiabatic explosion of a stoichiometric hydrogen−air mixture. The single line between 900 and 2000 K shows the exact matching of 10 lines. (a) Ratio $s_{H,k}/s_{H_2O,k}$. (b) Ratio $s_{OH,k}/s_{T,k}$.

Figure 5 shows that the ratio μ_{ikm} is not dependent on time for a very wide range of temperatures. Rabitz et al.[2,4] had a similar observation for the sensitivities of burner-stabilized flames, and they called this property *self-similarity*. However, the term self-similarity is widely used in another context in fractal theory; therefore, this notion will be called *global similarity* in this paper. This new term emphasizes that the value of μ_{ikm} is constant within a wide range of the independent variable.

Simultaneous existence of local and global similarities results in other identities. Local similarity means that the ratio of the sensitivities of two variables with respect to the same parameter is equal for any parameter:

$$\frac{s_{ik}(t)}{s_{jk}(t)} = \frac{s_{im}(t)}{s_{jm}(t)} \tag{8}$$

Rearranging it gives

$$\frac{s_{ik}(t)}{s_{im}(t)} = \frac{s_{jk}(t)}{s_{jm}(t)} = \mu_{km}(t) \tag{9}$$

That is, the ratio μ_{km} is independent of the variable investigated if local similarity is also valid.

In constrained temperature explosion simulations, the initial value problem (eq 1a) was solved and the variables included

the mass fractions of species only. Since temperature was not a variable in this case, no temperature sensitivity could be calculated. Although the calculated concentration−time curves were identical to the adiabatic explosion results, the sensitivities were different. At adiabatic calculations, a changed rate coefficient changed the heat release rate and therefore the calculated temperature, which in turn changed the rate of all temperature-dependent rate coefficients. If the temperature−time profile is fixed, a changed parameter can modify the rate of other reactions only via the altered concentrations. The temperature−time profile of the perturbed system will be identical to that of the unperturbed one, but because enthalpy is a function of temperature *and* concentrations, the enthalpy−time profile will be different.

Figure 6 shows the calculated sensitivities for the explosion of stoichiometric hydrogen−air mixtures in a constrained temperature simulation. The sensitivities of the mass fractions of hydrogen and water are plotted. The perfect order of Figure 1b and c is not apparent in this figure. The curves show some similarity, but plotting the ratio of them according to eq 3 reveals (see Figure 7) that the level of similarity has decreased. The sensitivity ratios for some of the parameters are nearly identical, indicating local similarity of the sensitivities of these parameters. Figure 7 also presents the ratio of the production rates of the hydrogen atom and water. It is clear that the scaling relation is

Similarity of Sensitivity Functions

J. Phys. Chem. A, Vol. 107, No. 13, 2003 **2221**
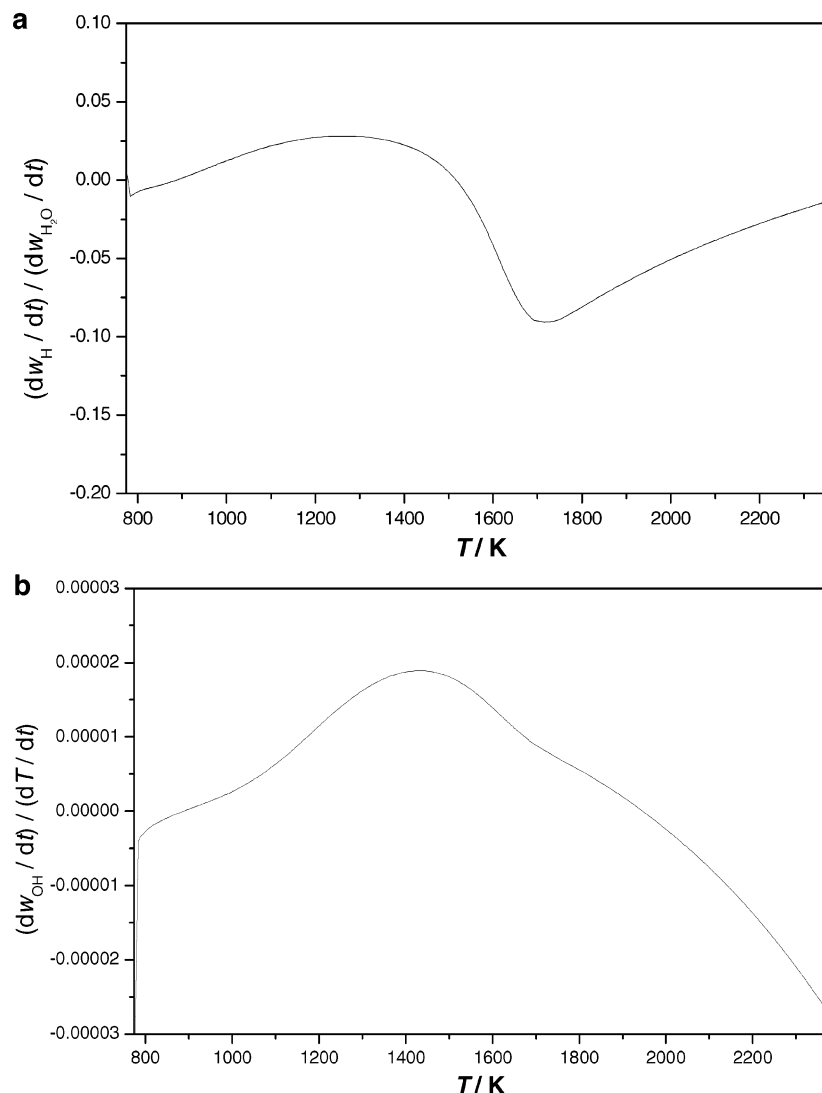
Figure 4. Ratio of the derivative of variables with respect to time as a function of temperature for adiabatic explosion of a hydrogen−air mixture. (a) Ratio $(dw_H/dt)/(dw_{H_2O}/dt)$. (b) Ratio $(dw_{OH}/dt)/(dT/dt)$. The plotted ratio is identical in a wide range of temperature to the ratio of the corresponding sensitivity coefficients (cf. Figure 3).

valid for none of the sensitivity ratios in this case. Global similarity was also checked for the constrained temperature explosion simulations. Global similarity is not valid at any temperature range for the sensitivities of the hydrogen atom (Figure 8a). The ratios of water sensitivities are constant in the temperature range 900−1400 K (Figure 8b), but the reason is that the original sensitivities were also independent of temperature in this region (see Figure 6b).

In most real-life chemical kinetic systems concentrations and temperature are spatially inhomogeneous and the change of them can be described by an appropriate system of partial differential equations (PDEs). Probably the most frequently simulated 1D reaction−diffusion systems are stationary premixed laminar flames. It is possible to create and investigate such *flat flames* in the laboratory, and the measured temperature and concentration profiles can be compared with the simulation results. The general form of the corresponding PDEs is given by

$$\mathbf{L}(\mathbf{Y},\mathbf{p}) = \mathbf{0} \tag{10}$$

where $\mathbf{L}$ is a second-order differential operator. The detailed description of operator $\mathbf{L}$ for laminar flames and the corresponding boundary conditions can be found in many articles (see e.g. refs 2, 5, and 11), and they are not reproduced here.

The sensitivity matrices can be calculated by solving the following equation:

$$\mathbf{0} = \bar{\mathbf{J}}\mathbf{S} + \bar{\mathbf{F}} \tag{11}$$

where $\bar{\mathbf{J}} = \partial\mathbf{L}/\partial\mathbf{Y}$ and $\bar{\mathbf{F}} = \partial\mathbf{L}/\partial\mathbf{p}$.

For the simulation of burner-stabilized flames, the temperature profile has no fixed point, but the mass flow rate is fixed and independent of parameters. For freely propagating flames, the flame speed and therefore the mass flow rate changes with parameters, but the location of the reference temperature point is fixed. This is the reason the sensitivity functions are different for these two types of flames, as is clear from the comparison of parts a and b of Figures 9−11. Not only the shapes are different, but also the sensitivities of the freely propagating flames are much smaller than those of the burner-stabilized flames. Local similarity and the scaling relation are shown in parts a and b of Figure 12 for freely propagating and burner-stabilized adiabatic flames, respectively. Neither similarity appears in the case of freely propagating flames, but for burner-stabilized flames for a group of parameters the scaling relation (and therefore local similarity) is valid.

In constrained temperature flame simulations the calculated species concentration profiles are identical to those of the
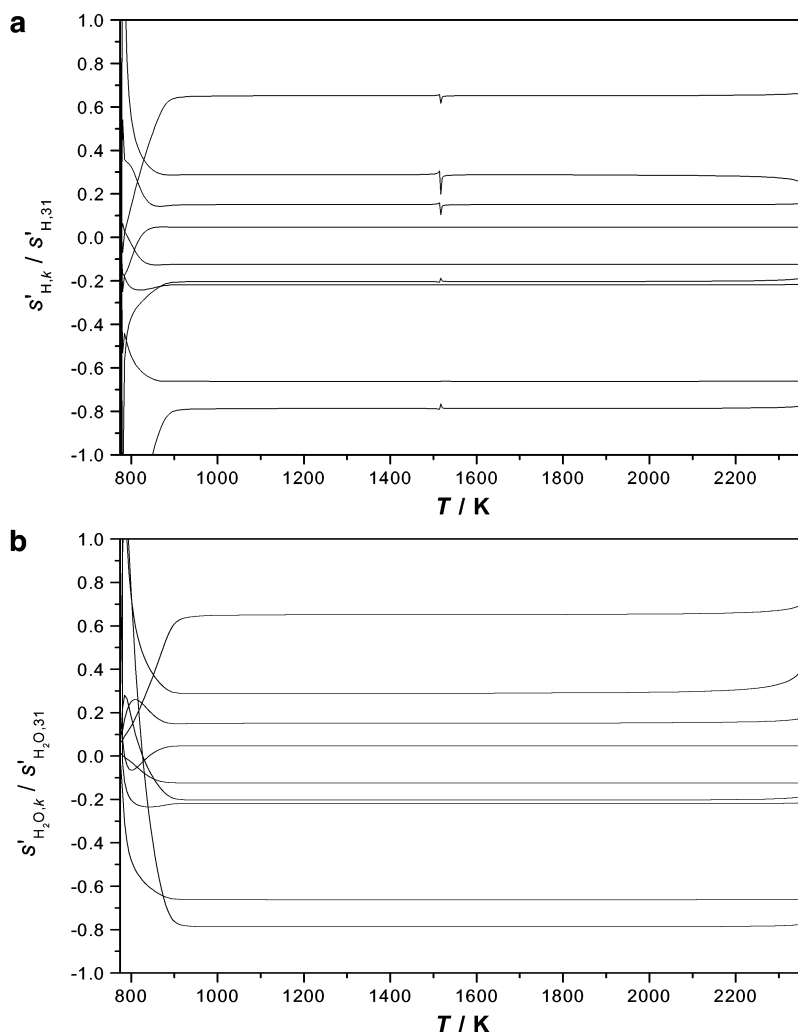
Figure 5. Ratio of sensitivity functions for the mass fractions of hydrogen and water with respect to two parameters as a function of temperature for adiabatic explosion of a stoichiometric hydrogen−air mixture. Here and in all the subsequent figures, s' indicates a seminormalized sensitivity coefficient, e.g., $s'_{H,k} = dw_H/d \ln A_k = A_k(dw_H/dA_k)$. (a) Ratio $s'_{H,k}/s'_{H,31}$; (b) ratio $s'_{H_2O,k}/s'_{H_2O,31}$. Parameter 31 is the preexponential factor of reaction $H + HO_2 \rightarrow 2OH$. In part a the small peaks appeared where both original sensitivity functions passed through zero.

adiabatic flames, but the sensitivities are different for reasons similar to those described for explosions. Figure 13 shows that local similarity and the scaling relation are not valid for constrained temperature freely propagating and burner-stabilized flames. For adiabatic flames, global similarity is checked by plotting the ratio of water sensitivities in parts a and b of Figures 14 for freely propagating and burner-stabilized flames, respectively. Similar plots are provided in Figures 15 for constrained temperature flames. Of these four cases, only adiabatic burner-stabilized flames show global similarity for some parameters, but only at temperatures below 1400 K.

The results of numerical experiments on models of hydrogen−air combustion can be summarized in the following way: There is perfect local similarity, scaling relation, and global similarity for adiabatic explosions only. Constrained temperature explosions show local similarity for some parameters. Scaling relation is not valid even for these sensitivity coefficients. Adiabatic burner-stabilized flames show all three types of similarity, but only for some parameters. No similarity was found for any freely propagating flames and for constrained temperature burner-stabilized flames.

These similarity relations are not features of the hydrogen combustion only. Figure 16 shows the values of λ_{ij} and μ_{km} as a function of temperature calculated for adiabatic methane−air

explosion. The plots demonstrate that local and global similarity are also present in this model, although it has many more variables and parameters.

4. Previous Results on the Similarity of Sensitivities

Reuven et al.[1] developed a computer code for the calculation of local sensitivities of stationary two-point boundary value problems. They tested the code on a simple model of 1D laminar flames for both burner-stabilized and freely propagating conditions. The chemistry included two first-order steps and three species: a reactant, an intermediate, and a product. The program calculated temperature, the concentrations of the three species, their local sensitivities, and also the elements of the Green's function matrix. The meaning of the Green's function is to be discussed in detail in section 6. In the burner-stabilized flame calculations of Reuven et al.,[1] the sensitivity curves of each variable with respect to all parameters as a function of distance were found to be very similar to each other. The Green's function elements changed little with the location of perturbation x' and were primarily determined by the temperature at position x. Therefore, they concluded that "the effect of parameter variations is channeled through the temperature in the present model", and this is the reason for the similarity of sensitivity−distance functions. In accordance, in freely propagating flame

Similarity of Sensitivity Functions

J. Phys. Chem. A, Vol. 107, No. 13, 2003 **2223**
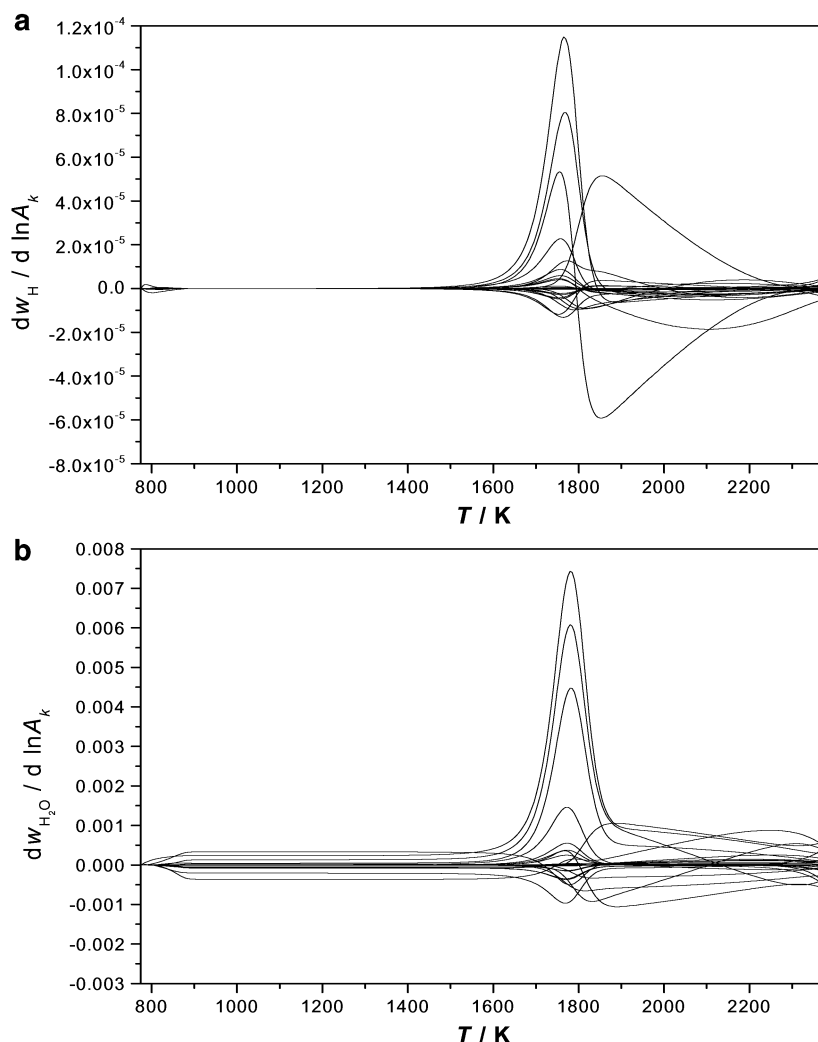
Figure 6. Sensitivities as a function of temperature calculated for the constrained temperature hydrogen−air explosion calculations. Sensitivity coefficients belonging to the mass fractions of (a) H and (b) H_2O are plotted.
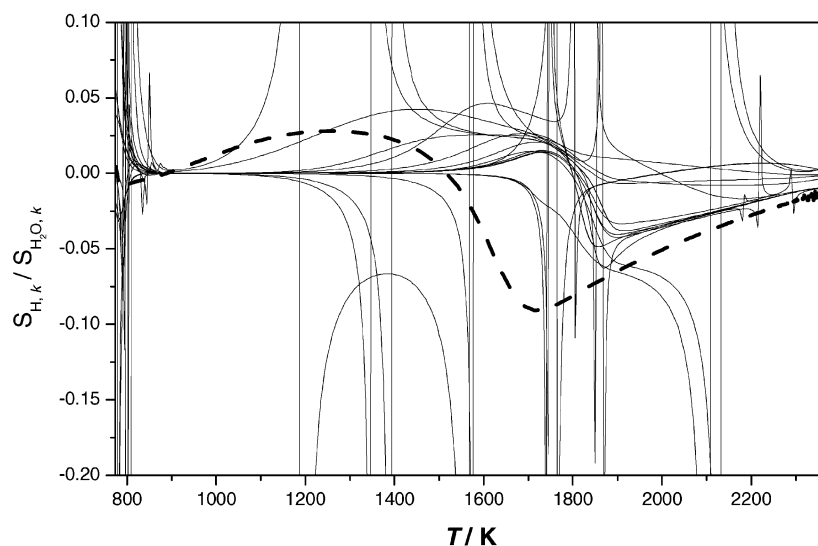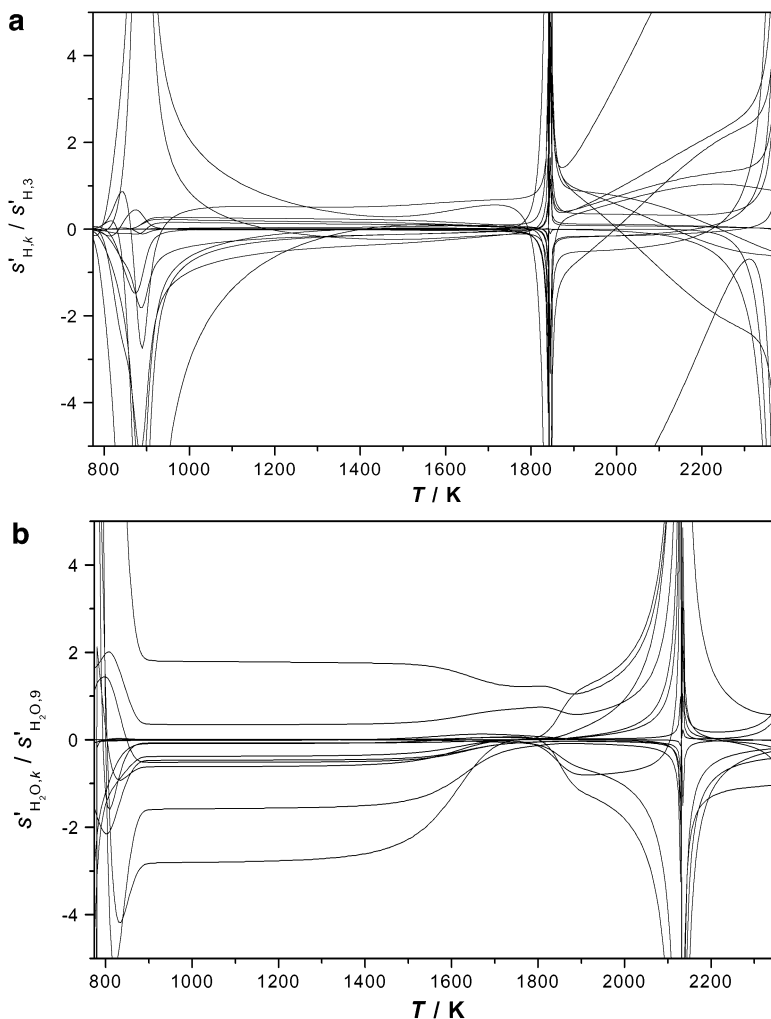

Figure 7. Ratio of sensitivity functions $s_{H,k}/s_{H_2O,k}$ for the constrained temperature explosion of a stoichiometric hydrogen−air mixture. Also, the ratio of the corresponding production rates $(dw_H/dt)/(dw_{H_2O}/dt)$ is plotted using a dashed line.

calculations not only was the sensitivity of calculated temperature zero at the point of the reference temperature but also the sensitivities of all other variables were also very small.

As a next step, Reuven et al.[2] applied the code for the calculation of sensitivities of premixed hydrogen−air flames.

They claimed that all results referred to freely propagating flames (see p 296), but in a later publication they clarified (ref 5, p 273) that the calculated sensitivities had belonged to adiabatic burner-stabilized flames. The temperature sensitivity−distance curves for the rate and diffusion coefficients were very

Figure 8. Ratio of sensitivity functions for the mass fractions of hydrogen and water with respect to two parameters as a function of temperature for constrained temperature explosion of a stoichiometric hydrogen−air mixture. (a) Ratio $s'_{H,k}/s'_{H,3}$. (b) Ratio $s'_{H_2O,k}/s'_{H_2O,9}$. Parameters 3 and 9 are the pre-exponential factors of reactions $H_2 + OH \rightarrow H_2O + H$ and $O_2 + H \rightarrow OH + O$, respectively.

similar to each other. The similarity was also present but was not so uniform for the HO_2 sensitivity profiles. They also calculated sensitivity functions for constrained temperature flames and claimed that "such a constrained calculation disallows the response of the species to parameter variations to be controlled by the temperature". These constrained temperature calculations produced less similar HO_2 sensitivity curves with respect to all parameters. For further theoretical explanation on similarity, they referred to the forthcoming Rabitz−Smooke paper.[4]

An article about the application of the code[3] for a $CO/H_2/O_2$ flame appeared in 1994, but most of the calculations seem to be completed earlier (see reference (Mishra et al., 1986) in article 2 and refs 5 and 46 in articles 4 and 5, respectively). Mishra et al. simulated a burner-stabilized wet carbon monoxide flame and plotted the sensitivity of the CO mole fraction with respect to the pre-exponential factors and the diffusion coefficients. The figures demonstrated the global similarity of the curves. Mishra et al. also reported the scaling relation to be valid. The calculations were repeated with a constrained temperature profile, and they concluded that "the loss of self-similarity behavior and lessening of the sensitivity to the reactions ... underscores the dominant role of temperature". They also noted that laboratory flames are simulated either with calculated temperature profiles or using a fixed, experimentally measured temperature profile, and they stated that, to avoid misinterpreta-

tion of the kinetic data, one has to keep in mind that in the two cases different reactions are important for the reproduction of experimental values.

The article of Rabitz and Smooke[4] was the first theoretical paper on the similarity of sensitivity functions. They claimed that the onset of scaling relation and global similarity could be explained by assuming that there is a single *dominant variable* in the system. A dominant variable has the following properties: changing the value of the dominant variable changes the values of all other variables, but perturbation of the value of a nondominant variable does not change directly the value of another nondominant variable. However, such a perturbation changes the value of the dominant variable and it changes the values of other variables. For example, temperature is a dominant variable in adiabatic combustion systems, because temperature "enters the problem exponentially whereas all other dependent variables (i.e., species) enter linearly or quadratically" (ref 3, p 250).

According to Rabitz and Smooke,[4] functional dependence between the dominant variable and the other variables can be described in the following way:

$$Y_i(z,\mathbf{p}) = F_i(Y_1(z,\mathbf{p})) \qquad (12)$$

where Y_1 is the dominant dependent variable, F_i is a function which is not dependent directly on z and $\mathbf{p}$, Y_i is any other
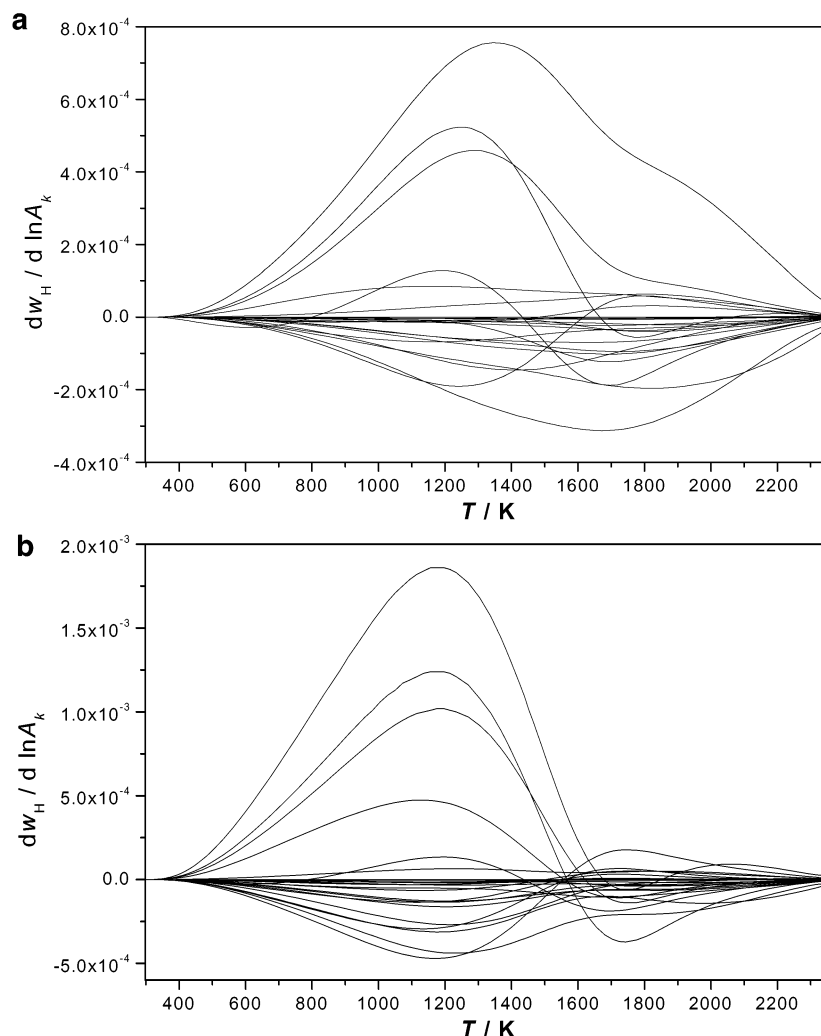
Similarity of Sensitivity Functions

J. Phys. Chem. A, Vol. 107, No. 13, 2003 **2225**
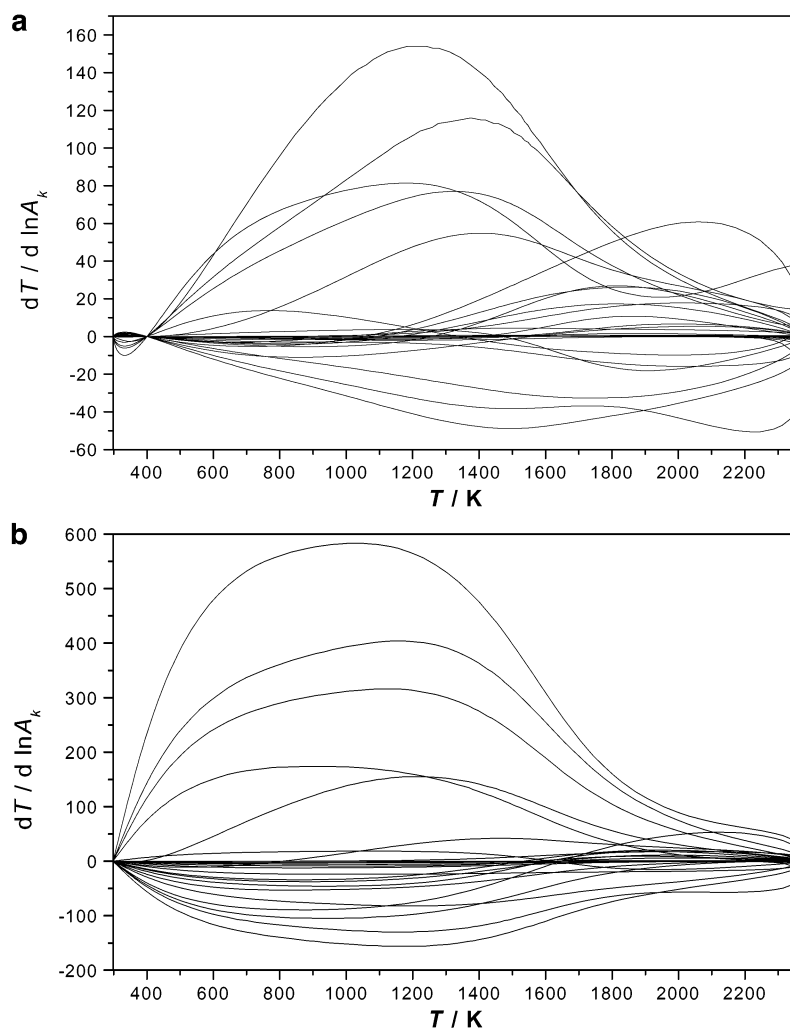
Figure 9. Sensitivities of temperature calculated for adiabatic stoichiometric hydrogen−air flames: (a) freely propagating and (b) burner-stabilized laminar flames.

variable, and z is the single independent variable (time or distance). In our opinion, eq 12 *is not* related to the presence of a dominant variable, because it contains no information about the consequence of variable perturbations. It only states that the value of Y_1 defines the values of all other variables. On the basis of eq 12, Rabitz and Smooke[4] proved the validity of the scaling relation for both the Green's and the sensitivity functions. Note, that Rabitz et al. published another article[18] on the study of the similarity of Green's functions. Rabitz also discussed the similarity of sensitivities in a review article on systems analysis.[19] He later demonstrated[17] that the scaling relation of sensitivity functions could be obtained without the prior calculation of the Green's function matrix. In the resulting equations for the scaling relation, the variable Y_1 does not have a unique role, which also questions the interpretation of Y_1 as a dominant variable in eq 12. We consider that the mathematical proof of Rabitz and Smooke is valid, but an entirely different interpretation of their derivation will be given in the next section.

In the remaining part of the Rabitz−Smooke paper, global similarity was derived from the scaling relation by making assumptions about the structure of the Green's function. This derivation implied that a condition of global similarity is the existence of scaling relation. The numerical examples were taken from articles 1−3, and the percentage error of the scaling relation was calculated. The typical error was about 6%. Global similarity was not demonstrated by plotting the ratio of eq 7, but the authors stated (p 1117) that the ratios investigated were

"nearly invariant to x on significant flame range". Interestingly, the authors mentioned (p 1118) that the similarity of sensitivity functions may be related to central manifold theory, but they did not follow this path.

All numerical examples in article 4 were related to stationary laminar flames, and this raises the question if sensitivity functions calculated for models of homogeneous explosions reveal similarity. Vajda et al.[5] investigated this topic by comparing sensitivity functions of models of adiabatic explosions and laminar flames of stoichiometric hydrogen−air mixtures. Temperature sensitivities of adiabatic explosions exhibited some global similarity, but no similarity was observed for the sensitivity of species. Existence of scaling relation was not investigated. The global similarity of the sensitivity functions of burner-stabilized laminar flames was reproduced. They concluded that "though the temperature is known to be a dominant variable in combustion processes, we show that only the simultaneous effects of thermal and transport phenomena change the form of the sensitivity functions significantly, leading to their self-similarity" (p 271). Figures 2 and 5 of this paper demonstrate that all sensitivity functions of models of the adiabatic hydrogen−air explosion show perfect global similarity. We repeated the calculations of Vajda et al.[5] using their mechanism and initial conditions; the calculated sensitivity functions showed perfect global similarity. Most likely the reason for the observed lack of similarity was having some numerical difficulties in their calculations. However, as a

Figure 10. Sensitivities of H mass fraction calculated for adiabatic stoichiometric hydrogen–air flames: (a) freely propagating and (b) burner-stabilized laminar flames.

consequence, until now nobody investigated the similarity of sensitivity functions of homogeneous kinetic systems.

Vajda and Rabitz[6] investigated thermal explosions modeled by a single step, nth-order, exothermic reaction. The model had two variables: temperature and the reactant concentration. Sensitivities with respect to the model parameters were calculated, and global similarity was observed for parameter sets where the model simulated thermal runaway. The authors stated that the onset of global similarity could be explained if the model has two properties: temperature is a dominant variable, and the sensitivity equations are pseudohomogeneous in a time window. The reasoning referred to their two-variable model, and it will be investigated, extended, and modified in section 6 of this paper.

5. Origin of Scaling Relation and Local Similarity

Mathematical models usually describe the cooperation of several physical processes, and these processes may have very different time scales. In chemical kinetics, this property was first met by Bodenstein,[20] who applied the quasi-steady-state approximation (QSSA) for the approximate analytical solution of systems of kinetic differential equations. An account of the history of the theoretical investigations of the QSSA was given in ref 21. Applicability of the QSSA is related to the stiffness of the kinetic ordinary differential equations (ODEs), which is caused by the very different eigenvalues of the Jacobian. In

general, the local time scales of models can be identified by the eigenvalue–eigenvector analysis of the Jacobian. This way n modes are related to a model of n variables and each mode has a local time scale, which may be different at another point of the variable space. If a mode is much slower than the time scale of our interest, it appears to be frozen. If a mode is much faster than our time scale, it causes algebraic relations among the variables. Lam and Goussis[22–24] built up a comprehensive kinetic analysis method based on the eigenvalue–eigenvector analysis of the Jacobian. They called the very slow modes (characterized by small absolute values of eigenvalues) *dormant modes* and the very fast modes (characterized by large negative eigenvalues) *exhausted modes*. The classical simplification procedures in chemical kinetics are examples of intuitive applications of different time scales: the pool concentration approximation is related to dormant modes, while fast equilibrium and quasi-steady-state approximations are related to the exhausted modes. Roussel and Fraser[25] investigated small enzyme kinetic systems and stated that the existence of very different time scales causes the trajectory of the solution to move on slow manifolds. Approaching the equilibrium point, the dimension of the manifold the trajectory moves on gradually decreases. In a dynamical system of n variables the degree of freedom of movement is originally $n_1 < n$, after deducing the conservation relations (like element conservations in closed systems) and the extremely slow dormant modes. Therefore,

Similarity of Sensitivity Functions

J. Phys. Chem. A, Vol. 107, No. 13, 2003 **2227**
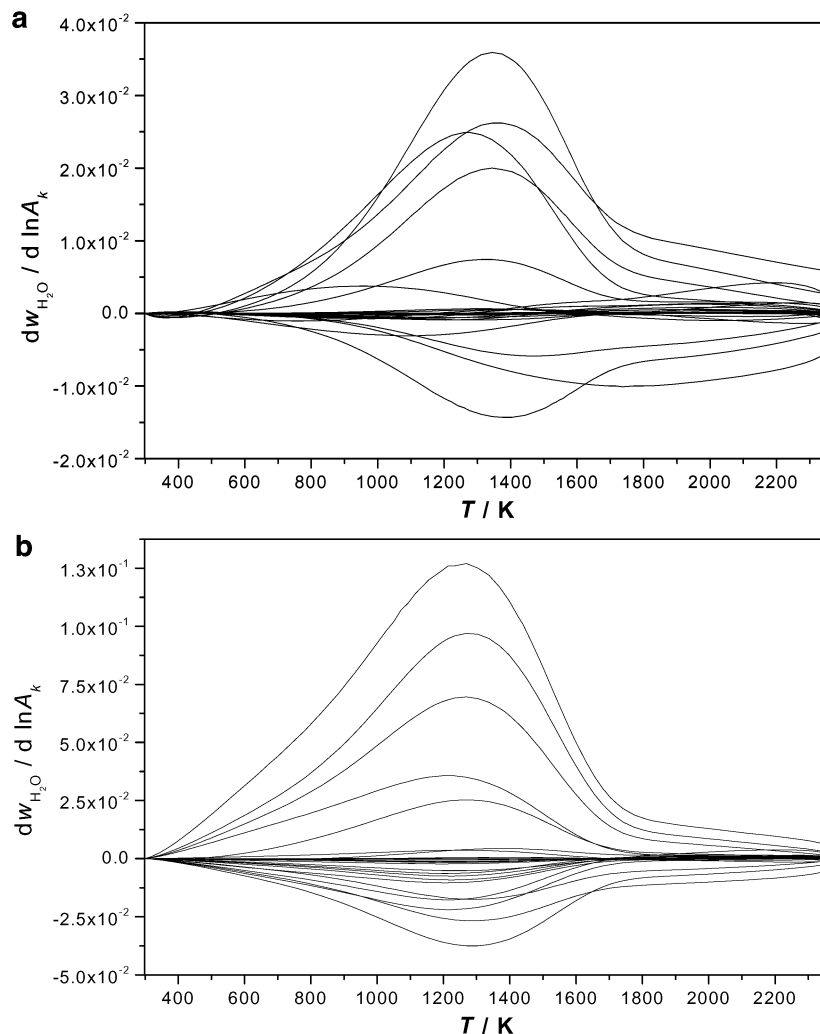
Figure 11. Sensitivities of H_2O mass fraction calculated for adiabatic stoichiometric hydrogen−air flames: (a) freely propagating and (b) burner-stabilized laminar flames.

the trajectory originally moves on an n_1-dimensional manifold, but as time advances, more and more modes become exhausted and finally the trajectory moves close to a two-dimensional surface (curved plate), then moves close to a one-dimensional curve, and finally arrives at the zero-dimensional equilibrium point if it exists. If the model is not required to describe the dynamics of the system at early times, a low-dimensional model (that is a model having few variables) provides an accurate description of the long-term dynamics. It is also possible that of the many modes only one coincides with our time scale; all other modes are either exhausted or dormant. In this case, the many-variable model can be replaced by an appropriate model having a single variable only.

Maas and Pope[26−28] elaborated algorithms and computer codes for the approximate numerical calculation of slow manifolds. A recent comparison of the method of Maas and Pope with that of Roussel and Fraser was given in ref 29. Maas and Pope also studied the existence of manifolds in several combustion models and generated reduced models having few variables only. They found that, at the adiabatic explosion of a CO−H_2−air mixture in a closed adiabatic vessel, after a very short time the trajectory moves close to a two-dimensional shell, then approaches a curve, and finally ends up at the equilibrium point. Eggels and de Goey[30] studied hydrogen−air combustion models and found that they could be described by a one-dimensional manifold, if the element composition and the

enthalpy of the gas were fixed. Büki et al.[31] also successfully simulated hydrogen−air explosions assuming that the trajectory moves close to a curved (1D) line.

In the description of slow manifolds, there are no distinguished variables: the manifolds can locally be parametrized by any nonconstant variable; global parametrization is possible by using continuously increasing variables, like water concentration in most combustion systems. If the element composition is fixed, the one-dimensional manifold (curve) belongs to a fixed enthalpy and another enthalpy invokes another curve.

The *scaling relation* can be explained on the basis of two assumptions: (i) the dynamical behavior of the system is controlled by a one-dimensional slow manifold in the space of variables; (ii) an infinitesimal change of a parameter changes the velocity of the movement on the manifold but negligibly dislocates the manifold. The proof below uses the derivation of Rabitz and Smooke,[4,17] but in the context of slow manifolds.

Let the one-dimensional manifold be defined by vector function **F**.

$$Y_i(z,\mathbf{p}) = F_i(Y_1(z,\mathbf{p})) \tag{13}$$

F_i defines the value of any variable Y_i as a function of the arbitrarily selected parametrizing variable Y_1. The letter z denotes the single independent variable (time or distance). The differential equations of the kinetic system are autonomous;
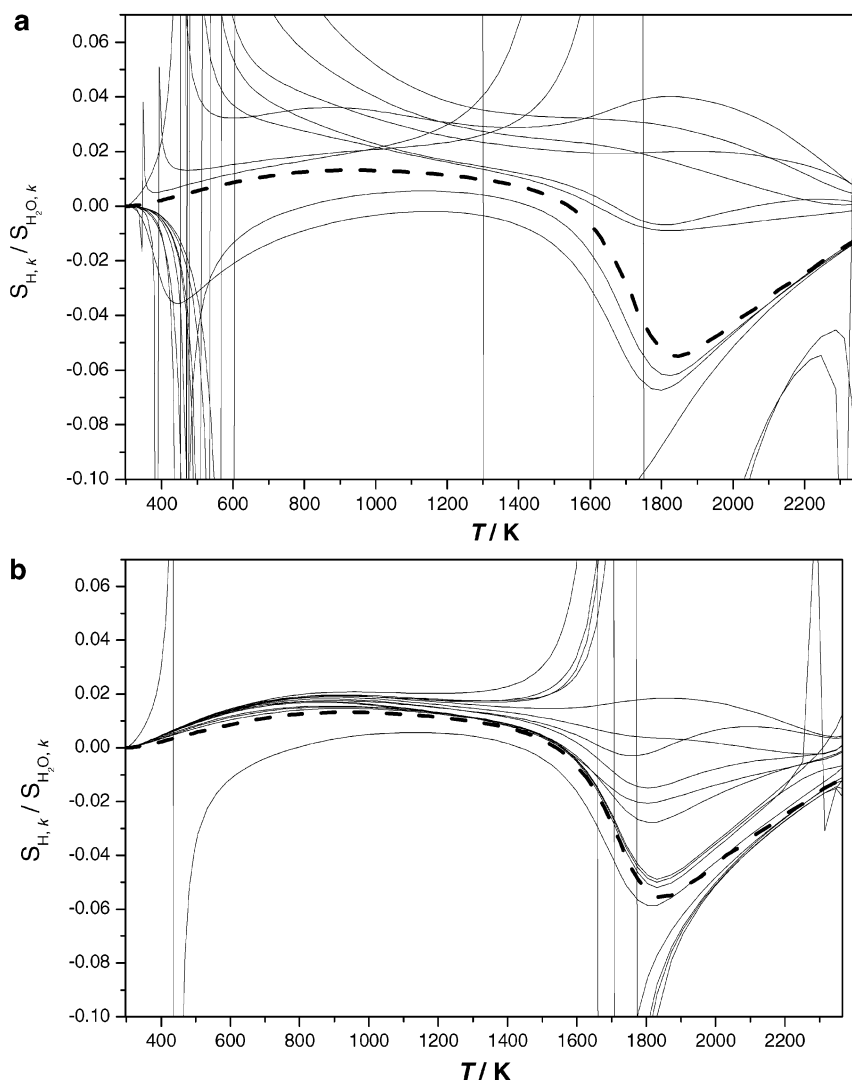
Figure 12. Ratios $s_{H,k}/s_{H_2O,k}$ and $(dw_H/dx)/(dw_{H_2O}/dx)$ for adiabatic stoichiometric hydrogen−air flames: (a) freely propagating and (b) burner-stabilized laminar flames.

therefore, F_i does not depend directly on z. Also, it can be assumed that a small change of parameters negligibly dislocates the manifold; therefore, the function F_i does not depend directly on $\mathbf{p}$. Differentiating eq 13 with respect to z gives

$$\frac{\partial Y_i(z,\mathbf{p})}{\partial z} = \frac{\partial F_i}{\partial Y_1}\frac{\partial Y_1(z,\mathbf{p})}{\partial z} \qquad (14)$$

while differentiating eq 13 with respect to any parameter p_j yields

$$\frac{\partial Y_i(z,\mathbf{p})}{\partial p_j} = \frac{\partial F_i}{\partial Y_1}\frac{\partial Y_1(z,\mathbf{p})}{\partial p_j} \qquad (15)$$

Combining the two gives a scaling relation:

$$\frac{\partial Y_i(z)}{\partial p_j} = \frac{\partial Y_1(z)}{\partial p_j}\frac{\partial Y_i}{\partial z}\left(\frac{\partial Y_1}{\partial z}\right)^{-1} \qquad (16)$$

This equation is valid for both temporal and 1D stationary systems and can easily be converted to other forms, given in eqs 6 and 8, that do not contain the variable Y_1. This also supports the claim that in eq 13 selection of the variable Y_1 is not unique. Equation 16 means that all other rows of the

sensitivity matrix can be obtained from any single row. Consequently, the rank of the sensitivity matrix is one.

In a similar way it can be shown that the dimension of the slow manifold determines the rank of the sensitivity matrix. An n-dimensional slow manifold can be parametrized by n variables for all variables $i = 1, ..., (N + 1)$.

$$Y_i(z,\mathbf{p}) = F_i(Y_1(z,\mathbf{p}),Y_2(z,\mathbf{p}),...,Y_n(z,\mathbf{p})) \qquad (17)$$

Differentiating it with respect to p_j:

$$\frac{\partial Y_i}{\partial p_j} = \left(\frac{\partial F_i}{\partial Y_1}\right)\left(\frac{\partial Y_1}{\partial p_j}\right) + \left(\frac{\partial F_i}{\partial Y_2}\right)\left(\frac{\partial Y_2}{\partial p_j}\right) + ... + \left(\frac{\partial F_i}{\partial Y_n}\right)\left(\frac{\partial Y_n}{\partial p_j}\right) \qquad (18)$$

The multiplicative factors $\partial F_i/\partial Y_1$, $\partial F_i/\partial Y_2$, ... are the same for all parameters; therefore

$$\mathbf{s}_i^T = \lambda_{i1}\mathbf{s}_1^T + \lambda_{i2}\mathbf{s}_2^T + ... + \lambda_{in}\mathbf{s}_n^T \qquad (19)$$

Therefore, the existence of an n-dimensional slow manifold invokes that the rank of the corresponding local sensitivity matrix is not greater than n, if the location of the manifold negligibly changes in the space of variables for small parameter perturbations.

Similarity of Sensitivity Functions

J. Phys. Chem. A, Vol. 107, No. 13, 2003 **2229**
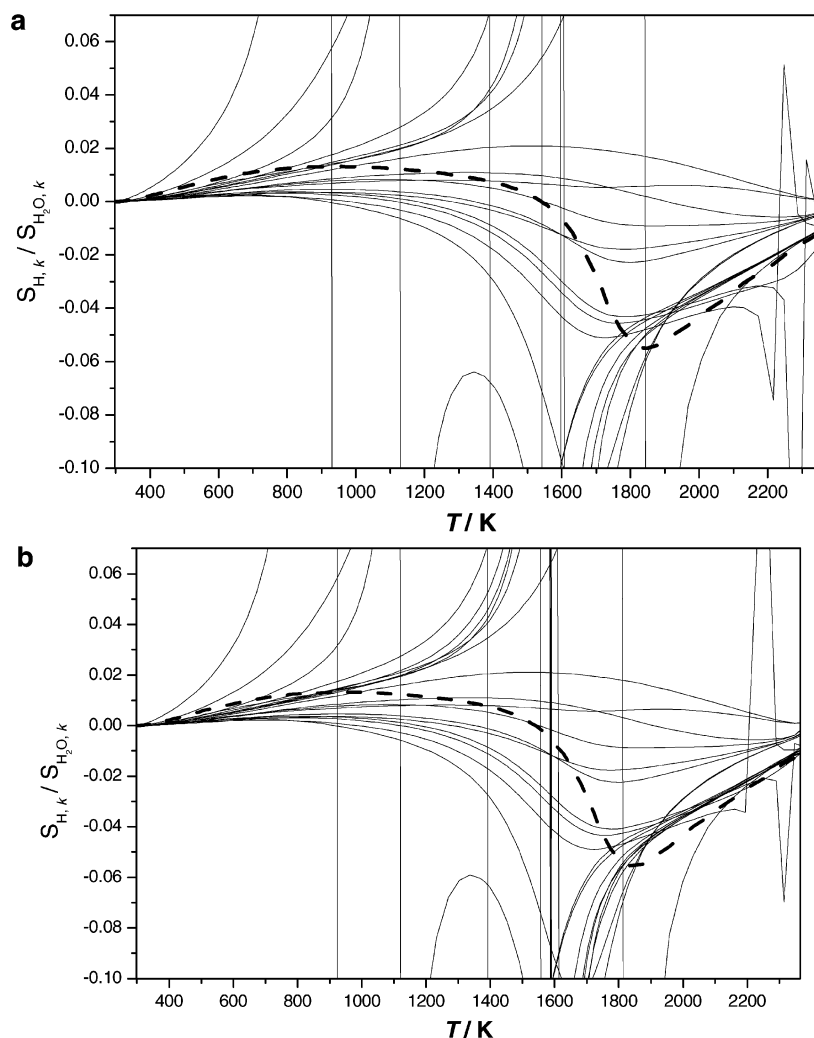
Figure 13. Ratios $s_{H,k}/s_{H_2O,k}$ and $(dw_H/dx)/(dw_{H_2O}/dx)$ for constrained temperature stoichiometric hydrogen–air flames: (a) freely propagating and (b) burner-stabilized laminar flames.

If local similarity exists for all pairs of sensitivity vectors, then any sensitivity vector can be obtained by multiplying any other nonzero sensitivity vector by a scalar (see eq 4). This is equivalent to the statement that the rank of the sensitivity matrix is one. If the rank of the sensitivity matrix is n, it might mean that local similarity is valid for none of the pairs of the sensitivity vectors. The other possible extreme is that eq 4 is valid for all sensitivity vectors but n. This can be the reason why, for example, for constrained temperature hydrogen explosions local similarity is valid for some of the parameters.

Relation of the dimension of slow manifolds with the scaling relation, local similarity, and the rank of the local sensitivity matrix can be justified also on the basis a geometrical description. Figure 17a is a schematic representation of a one-dimensional manifold. The space of variables is 10-dimensional in the case of a hydrogen–air explosion (9 species and temperature), but the schematic figure shows 3 axes only. Point **C** represents the actual status of the system and $\mathbf{E_0}$ is the equilibrium point that belongs to enthalpy h_0. The system moves with velocity vector $\dot{\mathbf{Y}}$ in the variable space. Projections of the velocity vector on the axes are the right-hand sides of eqs 1, which correspond to the production rates in chemical kinetics. The direction of the velocity vector is identical to the local direction of the manifold. If parameter p_k is changed infinitesimally, it only negligibly shifts the location of the manifold. However, since the location of the system at time t is obtained

by a long integration, the perturbed system will be close to point **C** but at a different **C′** location on the manifold. The direction of vector $\overrightarrow{\mathbf{CC′}}$ is also along the manifold for any parameter p_k perturbed; only the length of the vector will be different. Also, this direction will be identical for all sensitivity vectors $\partial\mathbf{Y}/\partial p_k$. Projections of this vector onto the axes will be $\{\partial Y_1/\partial p_k, \partial Y_2/\partial p_k, ..., \partial Y_n/\partial p_k\}$. If the directions of two vectors of any length are identical, the ratios of the projections to any two axes will also be identical. This explains the observed scaling relation, why any sensitivity vector can be obtained by multiplying any other sensitivity vector by a scalar (eq 4), and why the ratio of any pair of sensitivities is identical to the ratio of the corresponding production rates (eq 6).

The enthalpy of the system is preserved during an adiabatic simulation, even if the mechanism was modified by perturbing a kinetic parameter. However, in the constrained temperature simulations only the unperturbed system maintains the nominal enthalpy. Assume that the enthalpy of the unperturbed system is h_0, but because the perturbation modifies the concentrations but does not adjust the temperature accordingly, the perturbed system has a slightly different enthalpy at time t. The perturbed system will be at point **C′** on a different 1D manifold that belongs to enthalpy h_1. Perturbing another parameter will result in another state **C″**, having yet another enthalpy h_2 (see Figure 15c). The consequence is that constrained temperature calcula-
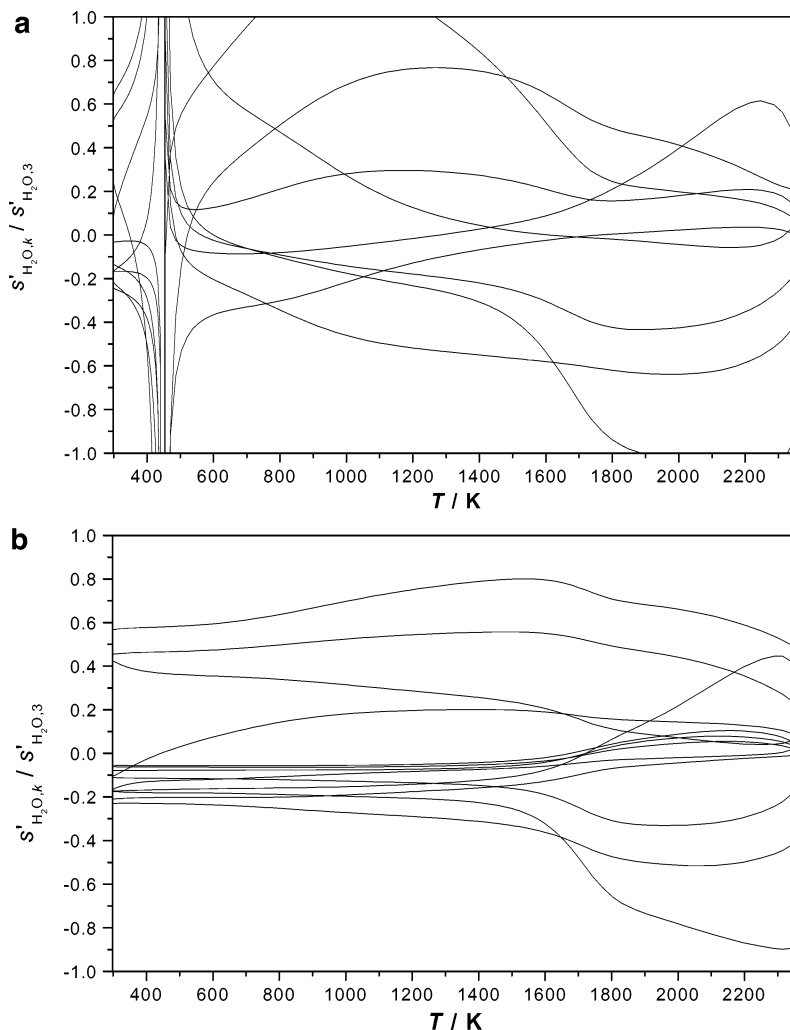
Figure 14. Ratio $s'_{H_2O,k}/s'_{H_2O,m}$ for adiabatic stoichiometric hydrogen−air flames: (a) freely propagating and (b) burner-stabilized laminar flames.

tions result in sensitivities that cannot be characterized by scaling relation.

If the dimension of the manifold is two, any rows of the sensitivity matrix can be obtained as a linear combination of two independent sensitivity vectors:

$$\mathbf{s}_i^T(t) = \lambda_{ij}(t)\,\mathbf{s}_j^T(t) + \lambda_{il}(t)\,\mathbf{s}_l^T(t) \qquad (20)$$

In this case, the velocity vector and the sensitivity vectors all fit onto a plane (see part d of Figure 17).

The rank of a square matrix is equal to the number of its nonzero eigenvalues, and the rank of a nonsquare matrix **M** is equal to the number of nonzero eigenvalues of matrix $\mathbf{M^T M}$. The sensitivity matrixes are calculated with numerical error; therefore, only an approximate rank can be calculated. Figure 18 shows the eigenvalues of the $\mathbf{S^T S}$ matrixes calculated for adiabatic and constrained temperature hydrogen−air explosion. In the case of the adiabatic explosion the sensitivity functions are very similar; therefore, one of the eigenvalues is 10^4 to 10^7 times larger than the second largest, and the rank of the sensitivity matrix is approximately one. In the case of constrained temperature hydrogen explosion there are six eigenvalues of similar magnitude, followed by a large gap. The rank of this sensitivity matrix is approximately six in a wide range of the independent variable.

Maas and Pope[27] demonstrated that concentration−distance profiles in laminar flames can be calculated by assuming that these are basically controlled by the slow manifold, determined by the chemical reactions, and perturbed by the diffusion of species and heat. Consider the concentrations in a 1D laminar flame as a curve in the space of variables, which is spanned between the points of the cold and hot boundary states. This curve practically coincides with the 1D manifold of hydrogen−air combustion above the temperature where the effect of chemical reactions is faster than that of diffusion, as is demonstrated in Figure 1. As previously, assume that the location of the curve in the space of variables does not change significantly due to an infinitesimal parameter perturbation. Let this curve be parametrized by physical distance. In burner-stabilized flames, changing a parameter changes the distance of the point of a given composition from the burner surface; that is, it changes the parametrization of the curve with distance. Then, reasoning similar to the case of homogeneous explosion explains the existence of the local similarity and scaling relation in burner-stabilized flames. However, due to the presence of diffusion, the sensitivities of burner-stabilized flames are expected to be less similar compared to those of the homogeneous explosions. In freely propagating flames, distance is measured from a point of the flame having the reference temperature. Perturbation changes the flame speed, and therefore the distance between the point of reference temperature and the other points of the flame does not change significantly. Consequently, local similarity and scaling relation cannot be observed among the sensitivity functions of freely propagating flames.

Similarity of Sensitivity Functions

J. Phys. Chem. A, Vol. 107, No. 13, 2003 **2231**
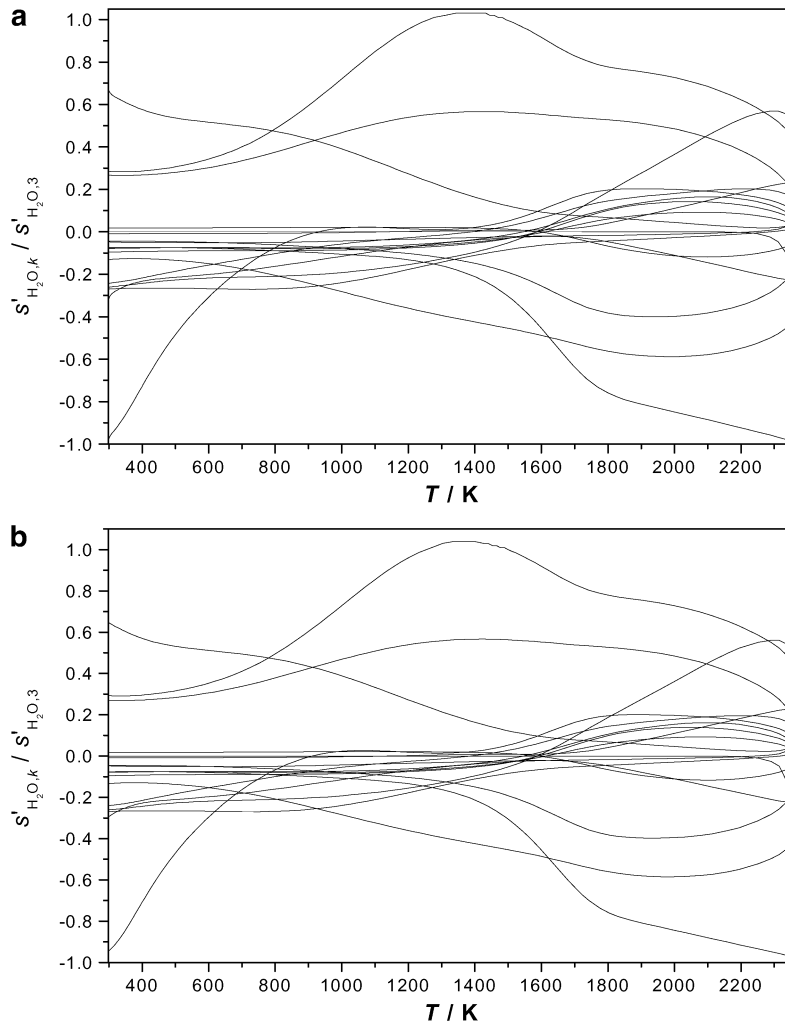
Figure 15. Ratio $s'_{H_2O,k}/s'_{H_2O,m}$ for constrained temperature stoichiometric hydrogen−air flames: (a) freely propagating and (b) burner-stabilized laminar flames.

Note that initial value sensitivities cannot be used for the investigation of manifolds. If an initial concentration is changed, it changes the enthalpy of the mixture and the element composition; therefore, the solution will run on a parallel manifold that the original system can never access.

6. Origin of Global Similarity

Vajda and Rabitz[6] have suggested that a necessary condition of global similarity is the pseudohomogeneity of the sensitivity differential equations and demonstrated it on the example of a single reaction step model of thermal explosion having two variables. Their derivation is extended and developed further in this section.

Consider first a spatially homogeneous, purely temporal system. The time history of the variables can be computed by solving the initial value problem

$$\frac{d\mathbf{Y}}{dt} = \mathbf{f}(\mathbf{Y},\mathbf{p}), \quad \mathbf{Y}(0) = \mathbf{Y}^0 \tag{21}$$

where $\mathbf{Y}$ is the $(N+1)$-vector of variables and $\mathbf{p}$ is the M-vector of parameters. Local sensitivities with respect to p_k can be calculated by solving the following initial value problem:

$$\frac{d}{dt}\frac{\partial \mathbf{Y}}{\partial p_k} = \frac{\partial \mathbf{f}}{\partial \mathbf{Y}}\frac{\partial \mathbf{Y}}{\partial p_k} + \frac{\partial \mathbf{f}}{\partial p_k}, \quad \frac{\partial \mathbf{Y}}{\partial p_k}(0) = \mathbf{0} \tag{22}$$

An alternative way is the calculation of the sensitivities via the Green's function matrix:

$$\frac{\partial \mathbf{Y}}{\partial p_k}(t) = \int_0^t \mathbf{G}(t,t') \frac{\partial \mathbf{f}}{\partial p_k}(t') \, dt' \tag{23}$$

The Green's functions can be obtained by solving the following initial value problem:

$$\frac{d}{dt}\mathbf{G}(t,t') = \frac{\partial \mathbf{f}}{\partial \mathbf{Y}}(t)\,\mathbf{G}(t,t'), \quad \mathbf{G}(t',t') = \mathbf{I} \tag{24}$$

where $\mathbf{I}$ is the $(N+1) \times (N+1)$ unit matrix and $\mathbf{G}(t,t')$ is the $(N+1) \times (N+1)$ Green's function matrix. An element of this matrix shows how the perturbation of Y_j at time t' influences Y_i at time t.

$$g_{ij}(t,t') = \frac{\partial Y_i(t)}{\partial Y_j^0(t')} \tag{25}$$

Let us calculate now the sensitivity of variable vector $\mathbf{Y}$ separately for time intervals $(0, t_1)$ and (t_1, t) using identity
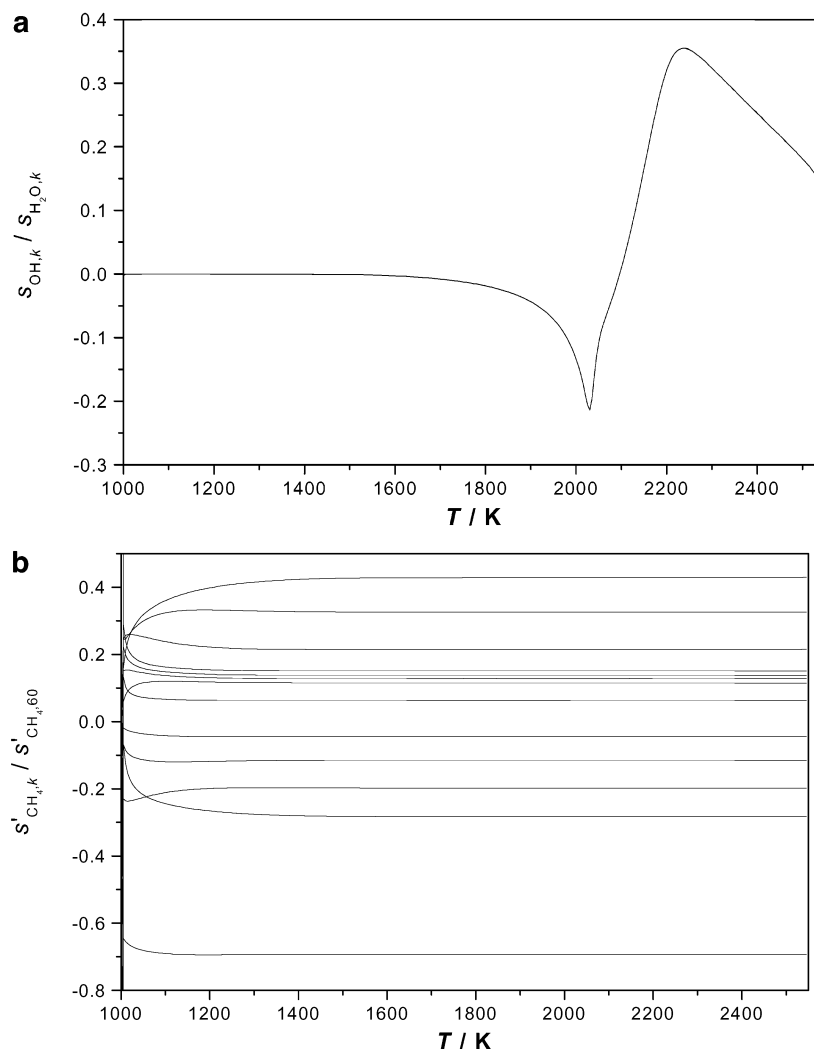
Figure 16. Ratio of sensitivities as a function of temperature calculated for an adiabatic methane−air explosion indicating local and global similarity. The initial conditions are a stoichiometric CH_4−air mixture, $p = 1$ bar, and $T^0 = 1000$ K.

$\mathbf{G}(t,t') = \mathbf{G}(t,t_1)\,\mathbf{G}(t_1,t')$:

$$\frac{\partial \mathbf{Y}}{\partial p_k}(t) = \int_0^{t_1} \mathbf{G}(t,t_1)\,\mathbf{G}(t_1,t')\,\frac{\partial \mathbf{f}}{\partial p_k}(t')\,dt' +$$
$$\int_{t_1}^{t} \mathbf{G}(t,t_1)\,\mathbf{G}(t_1,t')\,\frac{\partial \mathbf{f}}{\partial p_k}(t')\,dt' \quad (26)$$

Assume that $\partial \mathbf{f}/\partial p_k \approx \mathbf{0}$ in the time interval (t_1, t) and therefore the second term on the right-hand side of eq 26 can be neglected. The existence of the term $\partial \mathbf{f}/\partial p_k$ makes the sensitivity differential equation (eq 22) inhomogeneous. If this vector is nearly zero, then eq 22 is called pseudohomogeneous. Matrix $\mathbf{G}(t,t_1)$ is not a function of the variable of integration t'; therefore, for any $t > t_1$

$$\frac{\partial \mathbf{Y}}{\partial p_k}(t) = \mathbf{G}(t,t_1)\int_0^{t_1}\mathbf{G}(t_1,t')\,\frac{\partial \mathbf{f}}{\partial p_k}(t')\,dt' = \mathbf{G}(t,t_1)\,\frac{\partial \mathbf{Y}}{\partial p_k}(t_1) \quad (27)$$

Accordingly, sensitivity of variable i with respect to parameter k can be calculated by

$$\frac{\partial y_i}{\partial p_k}(t) = \sum_{j=1}^{N+1} g_{ij}(t,t_1)\,\frac{\partial y_j}{\partial p_k}(t_1) \quad (28)$$

If local similarity exists at time t_1, then the ratio of the

sensitivities of any pair of variables is independent of the parameter perturbed. Select an arbitrary variable h and substitute the local similarity relation $\partial y_j/\partial p_k = \lambda_{jh}(\partial y_h/\partial p_k)$ into eq 28:

$$\frac{\partial y_i}{\partial p_k}(t) = \frac{\partial y_h}{\partial p_k}(t_1)\sum_{j=1}^{N+1} g_{ij}(t,t_1)\,\lambda_{jh}(t_1) \quad (29)$$
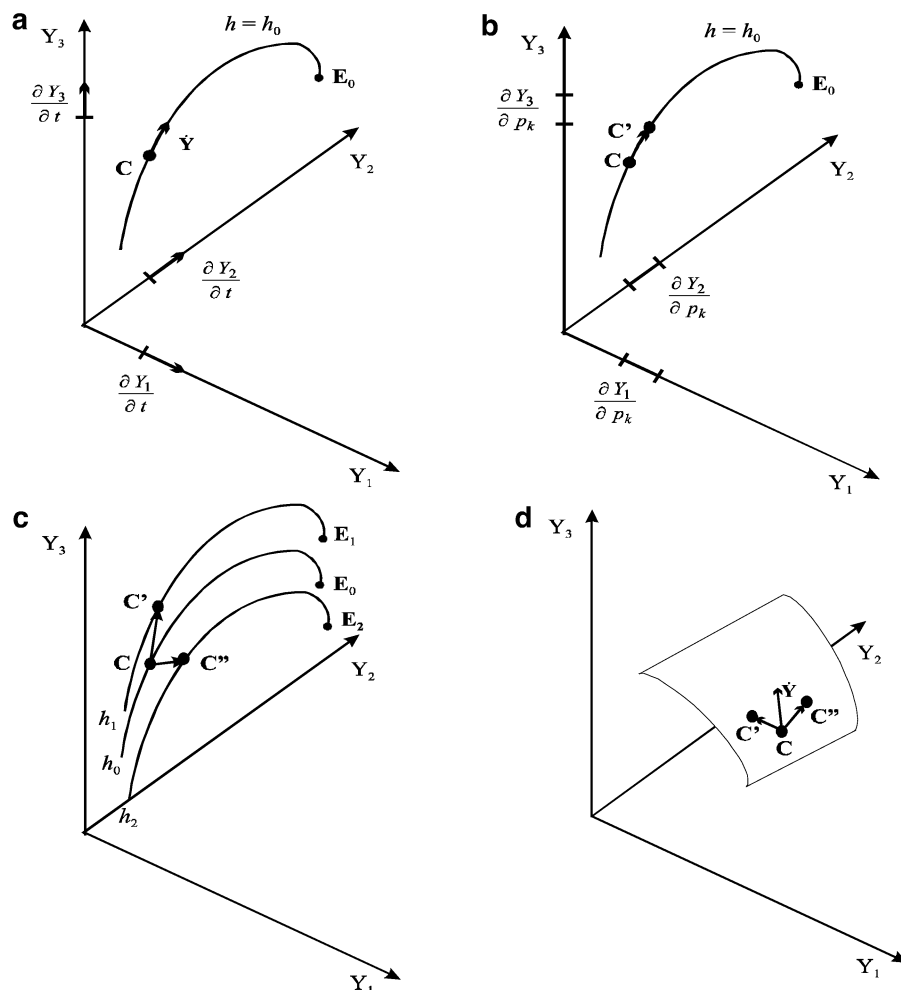
that is

$$\left(\frac{\partial y_i}{\partial p_k}(t)\right)\Big/\left(\frac{\partial y_h}{\partial p_k}(t_1)\right) = \sum_{j=1}^{N+1} g_{ij}(t,t_1)\,\lambda_{jh}(t_1) \quad (30)$$

Let us make a similar expression for another parameter m.

$$\left(\frac{\partial y_i}{\partial p_m}(t)\right)\Big/\left(\frac{\partial y_h}{\partial p_m}(t_1)\right) = \sum_{j=1}^{N+1} g_{ij}(t,t_1)\,\lambda_{jh}(t_1) \quad (31)$$

The right-hand sides of eqs 30 and 31 are equal, and the combination of the two equations gives

$$\frac{\dfrac{\partial y_i}{\partial p_k}(t)}{\dfrac{\partial y_i}{\partial p_m}(t)} = \frac{\dfrac{\partial y_h}{\partial p_k}(t_1)}{\dfrac{\partial y_h}{\partial p_m}(t_1)} = \mu_{km} \quad (32)$$

Similarity of Sensitivity Functions

J. Phys. Chem. A, Vol. 107, No. 13, 2003 **2233**

Figure 17. (a) One-dimensional manifold (curved line) in the space of variables, belonging to enthalpy h_0. Dot **C** represents the actual status of the system, dot $\mathbf{E_0}$ is the equilibrium point, and vector $\dot{\mathbf{Y}}$ is the velocity. Projections of the velocity vector on the axes are the RHS of the ODE (production rates in chemical kinetics). (b) Dot **C** represents the actual status of the system, and dot **C′** is the status of the system when parameter p_i has been infinitesimally perturbed. Because movement is possible only on the locally linear 1D manifold, the directions of the vectors $\dot{\mathbf{Y}}$, $\overline{\mathbf{CC'}}$, and $\partial\mathbf{Y}/\partial p_k$ are identical, and therefore the ratios of the coordinates of these vectors are identical for any pair of axes i and j and for any parameter k. (c) Bunch of one-dimensional manifolds in the space of variables belonging to enthalpies h_0, h_1, and h_2. If the parameter perturbation changes the enthalpy, the directions of vectors $\partial\mathbf{Y}/\partial p_k$ are different for different parameters p_k. (d) Two-dimensional manifold in the space of variables, belonging to enthalpy h_0. Dot **C** represents the actual status of the system, vector $\dot{\mathbf{Y}}$ is the velocity of movement of the actual state, and dots **C** and **C′** belong to perturbed parameter solutions with preserved enthalpy. The directions of the velocity and the sensitivity vectors no longer coincide, but they all fit onto a plane.

Equation 32 shows that the ratio of the two sensitivity coefficients at any time $t > t_1$ is independent of variable i and time; that is, the sensitivity functions are globally similar. The summary of eqs 26−32 is that if the system of sensitivity differential equations is pseudohomogeneous in time interval (t_1, t_2) and if local similarity exists at time t_1, then the sensitivity functions are globally similar in the time interval (t_1, t_2).

The reasoning above is different from the derivation of Vajda and Rabitz.[6] Their derivation, if generalized to arbitrary number of variables, is identical until eq 28. Vajda and Rabitz then assumed that one of the variables is dominant. Let variable h be dominant, which means that on the right-hand side of eq 28

$$g_{ih}(t,t_1)\frac{\partial y_h}{\partial p_k}(t_1) \gg \sum_{j=1, j\neq h}^{N+1} g_{ij}(t,t_1)\frac{\partial y_j}{\partial p_k}(t_1) \tag{33}$$

Consequently, all terms but that of the dominant variable can be neglected in eq 28:

$$\frac{\partial y_i}{\partial p_k}(t) = g_{ih}(t,t_1)\frac{\partial y_h}{\partial p_k}(t_1) \tag{34}$$

Applying it for another parameter m and combining the two equations gives

$$\frac{\dfrac{\partial y_i}{\partial p_k}(t)}{\dfrac{\partial y_i}{\partial p_m}(t)} = \frac{\dfrac{\partial y_h}{\partial p_k}(t_1)}{\dfrac{\partial y_h}{\partial p_m}(t_1)} = \mu_{km} \tag{35}$$

That is, a result identical to that of the previous reasoning was obtained. Ratio μ_{km} is independent of variable i; therefore, eq 35 means not only the existence of global similarity but also the existence of local similarity. Derivation of eqs 26−28 and 33−35 can be summarized that if the system of sensitivity differential equations is pseudohomogeneous and if a single dominant variable exists in the time interval (t_1, t_2), then the sensitivity functions show both global and local similarity in the time interval (t_1, t_2). Vajda and Rabitz[6] demonstrated in their
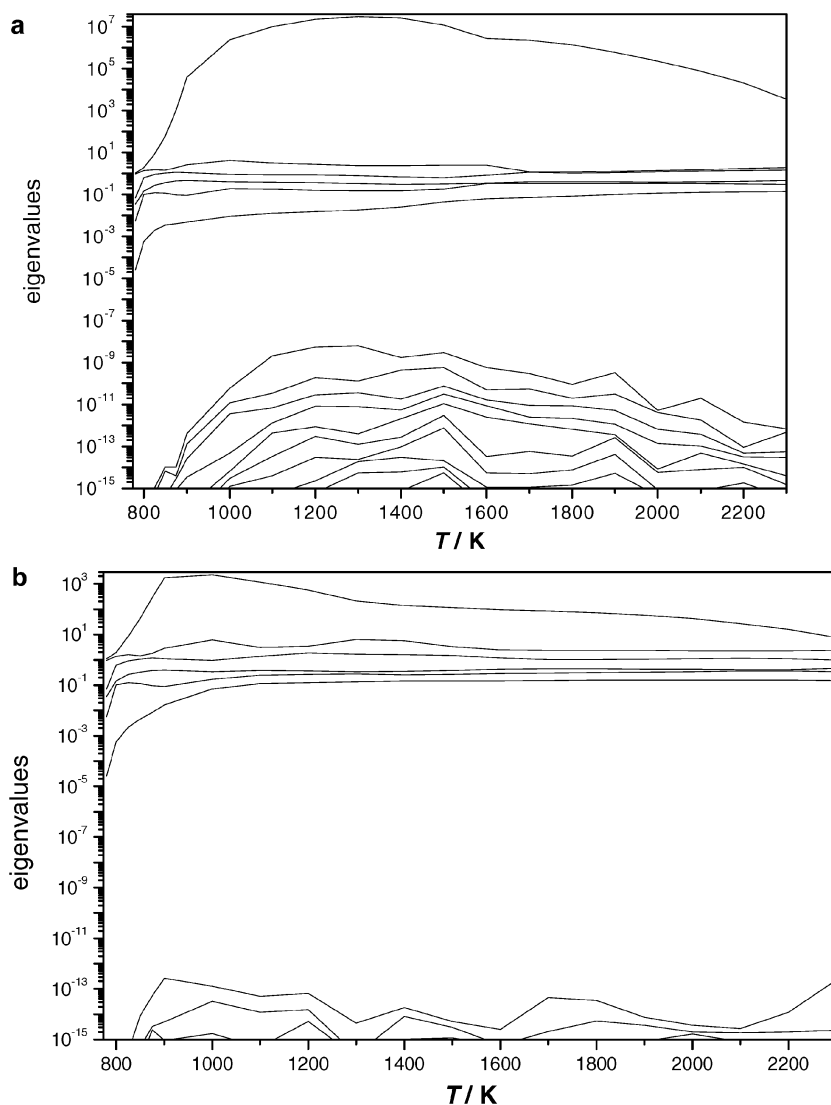
Figure 18. Eigenvalues of the $\mathbf{S}^T\mathbf{S}$ matrix as a function of temperature calculated for the (a) adiabatic and (b) constrained temperature hydrogen−air explosion calculations.
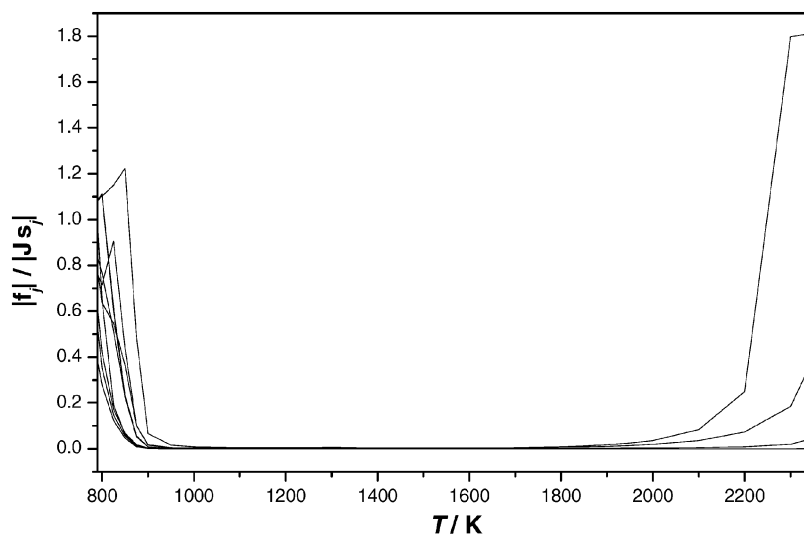
Figure 19. Inhomogeneous term is much smaller than the homogeneous term in the sensitivity differential equation during the adiabatic hydrogen−air explosion.

two-variable system that temperature is the dominant variable over the fuel concentration.

Every assumption of both derivations was checked numerically on the example of adiabatic hydrogen−air explosion.

Figure 19 shows that, in the window of global similarity in the system of sensitivity differential equations, the inhomogeneous term is negligible besides the homogeneous term; therefore, eq 22 is pseudohomogeneous. This was a necessary condition in

both derivations. Previously, the local sensitivities were calculated by the program SENKIN, which solves the sensitivity differential equations (eqs 22). Using a purpose written code, the Green's function matrix was calculated, and the sensitivities in temperature range 1000−2000 K were calculated in an entirely different way, using eq 27. The sensitivities calculated in the two ways agreed with good accuracy, which is not only a validation of eq 27 but also a successful test of both the sensitivity and Green's function matrix calculations. Therefore, all conditions of the first derivation were justified. In the next step, validity of eq 33 was tested. In Figure 20, the terms of eq 28 are compared. At none of the conditions investigated was the term belonging to temperature dominant over all other terms. In general, the terms belonging to radical concentrations were of similar importance to that of temperature. This indicates that *temperature is not a dominant variable* in the adiabatic hydrogen−air explosion system in the sense of eq 33. Consequently, the origin of global similarity cannot be explained by assuming that temperature is a dominant variable in the hydrogen combustion system. This statement is likely also valid for other combustion systems.

The derivation of global similarity for spatially one-dimensional stationary systems is similar, but not identical. Due to causality, in temporal systems perturbations have an influence on later events only. In 1D stationary systems, perturbation of parameters or variables at any position may have an influence on the values of variables at any other position due to the presence of diffusion.

Let the system be described by the following system of partial differential equations:

$$\mathbf{L}(\mathbf{Y},\mathbf{p}) = \mathbf{0} \tag{36}$$

where $\mathbf{L}$ is a second-order differential operator. The independent variable spans the range $[0, C]$. Knowing the boundary conditions, the spatial profiles of dependent variables can be calculated, and the sensitivity matrix functions are obtained by solving the following equations:

$$\mathbf{0} = \frac{\partial \mathbf{L}}{\partial \mathbf{Y}} \frac{\partial \mathbf{Y}}{\partial p_k} + \frac{\partial \mathbf{L}}{\partial p_k} \tag{37}$$

An alternative way is the calculation of the sensitivities via the Green's function matrix:

$$\frac{\partial \mathbf{Y}}{\partial p_k}(x) = \int_0^C \mathbf{G}(x,x') \frac{\partial \mathbf{L}}{\partial p_k}(x') \, dx' \tag{38}$$

The Green's functions can be obtained by solving the following initial value problem:

$$0 = \frac{\partial \mathbf{L}}{\partial \mathbf{Y}}(x) \, \mathbf{G}(x,x') + \mathbf{I}\,\delta(x - x'), \quad \mathbf{G}(x',x') = \mathbf{I} \tag{39}$$

where $\delta(x - x')$ is the Dirac delta function, $\mathbf{I}$ is the $(N + 1) \times (N + 1)$ unit matrix, and $\mathbf{G}(x,x')$ is the $(N + 1) \times (N + 1)$ Green's function matrix. An element of this matrix shows the change of the value of variable Y_i at distance x if the flux δJ_j perturbs the value of Y_j at distance x'.

$$G_{ij}(x,x') = \frac{\delta Y_i(x)}{\delta J_j(x')} \tag{40}$$

Let's calculate now the sensitivities separately for intervals (0, A), (A, B), and (B, C) and use the identities $\mathbf{G}(x,x') = \mathbf{G}(x,A)\,\mathbf{G}(A,x')$ and $\mathbf{G}(x,x') = \mathbf{G}(x,B)\,\mathbf{G}(B,x')$
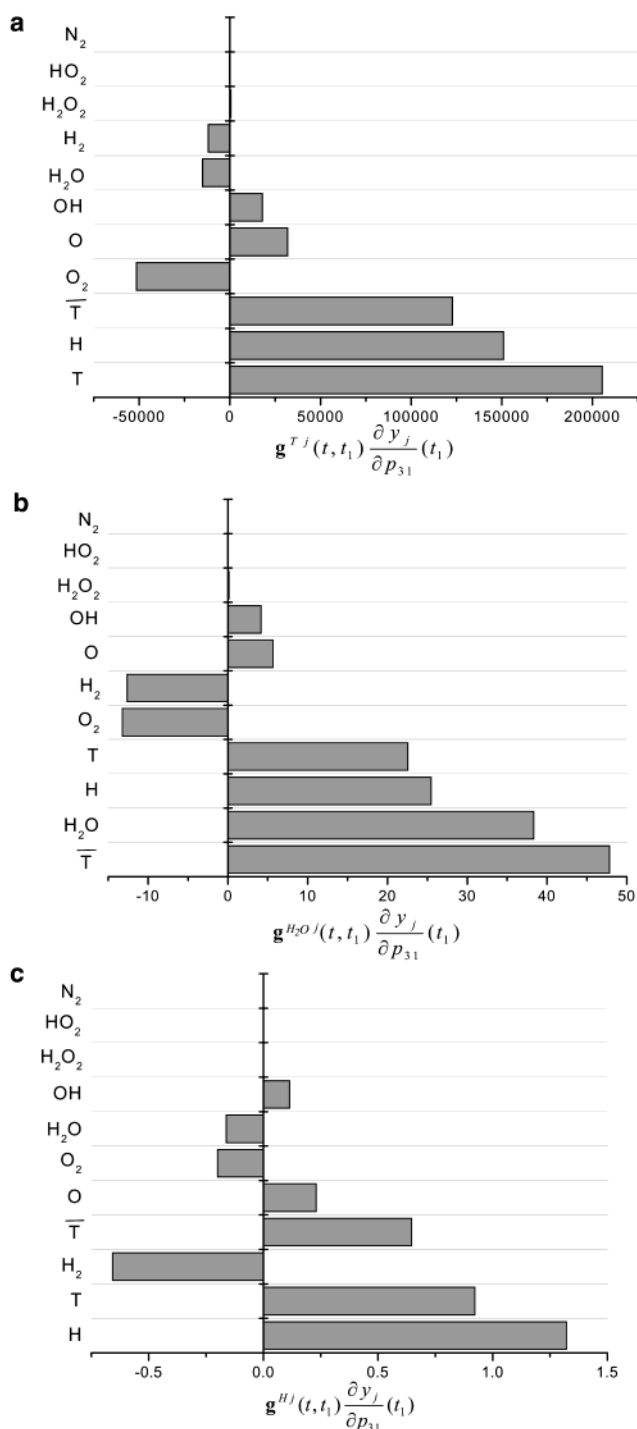
Figure 20. Comparison of the main terms of eq 28 in the calculation of the sensitivity of (a) temperature, (b) water mass fraction, and (c) mass fraction of hydrogen atom. Times t_1 and t correspond to mixture temperatures 1200 and 1400 K, respectively. The contribution denoted by T belongs to the term calculated from temperature sensitivity. The line denoted by $\bar{\text{T}}$ represents the sum of all terms minus the term of temperature sensitivity. The bars indicate that temperature is an important variable, but not the single dominant variable for adiabatic hydrogen−air explosions.

$$\frac{\partial \mathbf{Y}}{\partial p_k}(x) = \int_0^A \mathbf{G}(x,A)\,\mathbf{G}(A,x')\frac{\partial \mathbf{L}}{\partial p_k}(x')\,dx' +$$
$$\int_A^B \mathbf{G}(x,x')\frac{\partial \mathbf{L}}{\partial p_k}(x')\,dx' + \int_B^C \mathbf{G}(x,B)\,\mathbf{G}(B,x')\frac{\partial \mathbf{L}}{\partial p_k}(x')\,dx' \tag{41}$$

Assume that $\partial \mathbf{L}/\partial p_k \approx \mathbf{0}$ in spatial interval (A, B).

2236 *J. Phys. Chem. A, Vol. 107, No. 13, 2003*

Zsély et al.

$$\frac{\partial \mathbf{Y}}{\partial p_k}(x) = \int_0^A \mathbf{G}(x,A)\, \mathbf{G}(A,x')\, \frac{\partial \mathbf{L}}{\partial p_k}(x')\, dx' +$$

$$\int_B^C \mathbf{G}(x,B)\, \mathbf{G}(B,x')\, \frac{\partial \mathbf{L}}{\partial p_k}(x')\, dx' \quad (42)$$

$$\frac{\partial \mathbf{Y}}{\partial p_k}(x) = \mathbf{G}(x,A)\int_0^A \mathbf{G}(A,x')\, \frac{\partial \mathbf{L}}{\partial p_k}(x')\, dx' +$$

$$\mathbf{G}(x,B)\int_B^C \mathbf{G}(B,x')\, \frac{\partial \mathbf{L}}{\partial p_k}(x')\, dx' \quad (43)$$

$$\frac{\partial \mathbf{Y}}{\partial p_k}(x) = \mathbf{G}(x,A)\, \frac{\partial \mathbf{Y}}{\partial p_k}(A) + \mathbf{G}(x,B)\, \frac{\partial \mathbf{Y}}{\partial p_k}(B) \quad (44)$$

As before,

$$\frac{\partial y_i}{\partial p_k}(x) = \sum_{j=1}^{N+1} g_{ij}(x,A)\, \frac{\partial y_j}{\partial p_k}(A) + \sum_{j=1}^{N+1} g_{ij}(x,B)\, \frac{\partial y_j}{\partial p_k}(B) \quad (45)$$

If local similarity exists at distances A and B, then $\partial y_j/\partial p_k = \lambda_{jh}(\partial y_h/\partial p_k)$ for any arbitrarily selected variable h.

$$\frac{\partial y_i}{\partial p_k}(x) = \frac{\partial y_j}{\partial p_k}(A)\sum_{j=1}^{N+1} g_{ij}(x,A)\, \lambda_{jh}(A) + \frac{\partial y_j}{\partial p_k}(B)\sum_{j=1}^{N+1} g_{ij}(x,B)\, \lambda_{jh}$$

$$(B) \quad (46)$$

Unlike in temporal systems, global similarity will not be noticed if both neighboring regions have influence on the pseudohomogeneous region. In the case of flames, in the postflame region the variables are not very sensitive to the perturbation of rate parameters. Global similarity can be obtained if one of the terms on the right-hand side of eq 46 is neglected. Steps similar to the temporal case lead to

$$\frac{\dfrac{\partial y_i}{\partial p_k}(x)}{\dfrac{\partial y_i}{\partial p_m}(x)} = \frac{\dfrac{\partial y_h}{\partial p_k}(A)}{\dfrac{\partial y_h}{\partial p_m}(A)} = \mu_{km} \quad (47)$$

Equation 47 shows that the ratios of sensitivities s_{ik} and s_{im} are independent of variable i and distance; therefore, the sensitivity functions are globally and locally similar. The presence of diffusion means that perturbation of parameters in both intervals $(0, A)$ and (B, C) may have an effect on the value of variables in interval (A, B) and, therefore, weaken global similarity compared to the purely temporal case. If the system of sensitivity differential equations is pseudohomogeneous in distance interval (A, B), if local similarity exists at any side of this interval, and if the influence of parameter perturbation on the other side on variables in interval (A, B) is negligible, then the sensitivity functions in this interval become globally and locally similar.

7. Importance of the Similarity of Sensitivities

Global similarity of sensitivity functions means that the effect of the simultaneous change of several parameters can be fully compensated *for all variables*, in a wide range of the independent variable by changing a single parameter. Figure 21 shows the result of a numerical experiment. First, concentration profiles of H and H_2O were calculated in adiabatic explosion of a stoichiometric hydrogen−air mixture. Then, pre-exponential factors of four reactions ($O_2 + H + M \rightarrow HO_2 + M$, $H + HO_2 \rightarrow H_2 + O_2$, $O_2 + H \rightarrow OH + O$, and $H_2O + H \rightarrow H_2 + OH$) were increased by 1%, which changed the concentration profiles.

Due to the global similarity of sensitivities, changing a single parameter can tune back all concentration profiles simultaneously. In this case the pre-exponential factor of the reaction $H + HO_2 \rightarrow 2OH$ was increased by 0.5%.

In the case of empirical models, the only task of the model is to provide a good description of the observations. The presence of global similarity means that different parameter sets can provide the same simulation results. In the case of physical models, all parameters are assumed to have a "true" value. Perfect agreement between the experimental and the simulation results for all variables in a wide range of time (distance) is usually considered to be a proof that all used parameters are correct. Existence of global similarity means that if the values of some of the parameters are wrong, it can be fully masked by other parameters being also incorrect. If a physical parameter is determined in such a system by fitting to experimental data, error in the fixed parameter values causes the determined parameter to become erroneous. However, the fitted model perfectly reproduces all the experimental data, even if the values of several variables are measured at several time points (distances).

In the case of chemical kinetic models, existence of the similarity of sensitivity functions seems commonplace. This can be the reason complex reaction mechanisms can reproduce all available bulk experimental data by tuning only a few rate parameters. Also, very different reaction mechanisms exist in the literature that describe the same set of experimental data with a similar level of accuracy. This observation has been noted in the case of methane oxidation mechanisms[7] and mechanisms for NO_x chemistry in flames.[32]

In this paper, similarity of sensitivities was discussed in conjunction with chemical kinetic models. However, all derivations and statements are valid for any mathematical model, described by differential equations.

Smith and Szathmáry[33] have called attention to the similarity between flames and living organisms. Both consume food (fuel), transform it, and emit the end products. Laminar flames and living organisms both have complex self-stabilizing internal structures. Living organisms have to be robust, which means that even if some of the parameters (e.g. temperature, pH, salt concentration) change, the destabilizing effect has to be compensated in such a way that the values of *all* critical variables are restored simultaneously *everywhere* in the spatial domain of the living organism by changing a few internal parameters only. The explanation of the origin of global similarity in flames and other chemical kinetic systems may be used for models of the regulatory systems of living organisms to understand their remarkable robustness.

8. Conclusions

Most simulation programs in reaction kinetics calculate local sensitivity coefficients $s_{ik}(t) = \{\partial Y_i/\partial p_k\}$, which show the change of model result Y_i at time t if parameter p_k has slightly been changed. In the case of a general mathematical model, no relation is expected between the rows and columns of the sensitivity matrix $\mathbf{S}$ at any time. However, in some systems the following similarities were observed: (i) For *local similarity*, the value $\lambda_{ij}(t) = s_{ik}(t)/s_{jk}(t)$ depends on time and the model results Y_i and Y_j selected, but is independent of parameter p_k perturbed. (ii) For *scaling relation*, the ratio $\dot{Y}_i(t)/\dot{Y}_j(t) = s_{ik}(t)/s_{jk}(t)$ holds at any time and for any parameter p_k. The existence of a scaling relation means the presence of local similarity, but local similarity may exist without scaling relation. (iii) For *global similarity*, the value $\mu_{kl} = s_{ik}(t)/s_{il}(t)$ is independent of time (within an interval) and the model output studied.

Similarity of Sensitivity Functions

J. Phys. Chem. A, Vol. 107, No. 13, 2003 **2237**
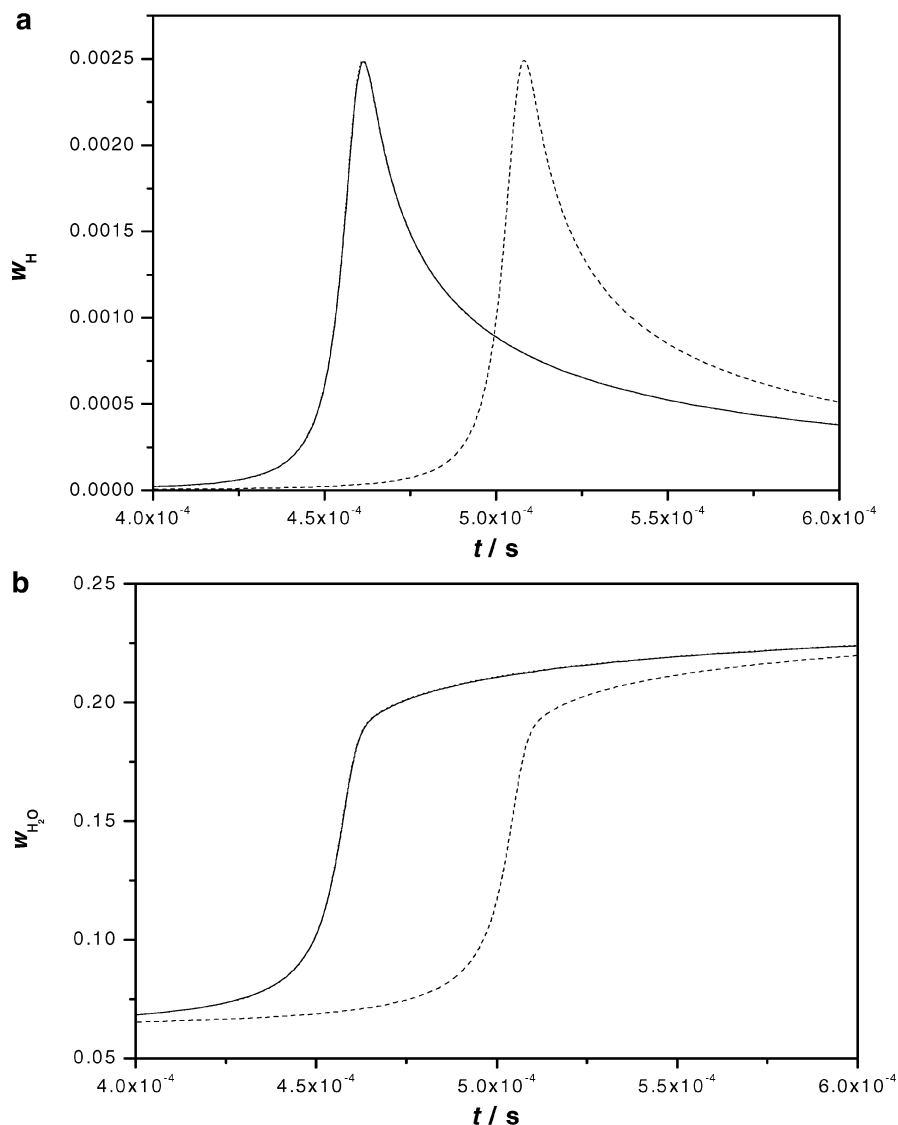
Figure 21. Simulation of parameter estimation in a system having global similarity. Calculated mass fraction−time curves of species H and H_2O in adiabatic hydrogen−air explosion: continuous line, the original model; dashed line, modified mechanism when the pre-exponential factors of four reactions are increased; dotted line (coincides with the continuous line), the same modified mechanism but the pre-exponential factor of a fifth reaction is also modified (for details see text).

The above types of similarities may exist in 1D stationary reaction−diffusion systems, like stationary laminar flames. In this case the independent variable is the distance, and in the scaling relation equation, the ratio of concentration gradients should be calculated.

One of the features of most chemical kinetic models is the existence of a very wide range of time scales. As a result, the dynamical dimension of the model is smaller than the number of variables, which means that the dynamics of the model is dictated by the low-dimensional manifold present. Assume now that this manifold is negligibly dislocated due to a small change of the parameter values. It has been demonstrated that if the dynamics of the system is ruled by a one-dimensional slow manifold, then scaling relation should be present. If the dimension of the manifold is n, then the approximate rank of the sensitivity matrix is not more than n. This latter may result in local similarity relations for some of the parameters.

Perturbation of a parameter results in changes in the values of some system variables, but the interdependence of the variables induces further modifications of the variable values. The second term on the right-hand side of the sensitivity differential equations (eqs 2) refers to the direct effect of parameter perturbations, and the first term is related to the indirect effect. The sensitivity differential equations are called pseudohomogeneous in a window of the independent variable, if here the direct effect on the change of sensitivity coefficients is negligible compared to the indirect effect. It has been shown that the pseudohomogeneous property of sensitivity differential equations and the presence of local similarity together imply global similarity. Global similarity was observed at the adiabatic explosions of hydrogen−air and methane−air mixtures, and approximate global similarity was found in a distance window in the burner-stabilized hydrogen−air flame.

Previously, scaling relation and global similarity were assumed to be a consequence of the presence of a single dominant variable in the system. For example, temperature was assumed to be such a variable in adiabatic combustion models. In this paper we have shown that these similarity features can be deduced without using the notion of dominant variable. Moreover, comparison of the terms of eq 28 indicated that temperature is not a single dominant variable in the case of the adiabatic explosion of hydrogen−oxygen mixtures, but for example, radical concentrations also have a high influence on the behavior of the system.

2238 *J. Phys. Chem. A, Vol. 107, No. 13, 2003*

Zsély et al.

The presence of local similarity, scaling relation, and global similarity usually has not been investigated in the study of chemical kinetic systems. Low-dimensional manifolds are present in most chemical kinetic models; therefore, local similarity of sensitivity functions is probably a general feature of these models. Very little is known about what conditions make the sensitivity equations become pseudohomogeneous. The calculations of Vajda and Rabitz[6] indicated that pseudohomogeneity might be present in thermal and autocatalytic runaway systems. However, pseudohomogeneity and therefore global similarity might appear also under other conditions. In some publications, plots of sensitivity functions showing global similarity appeared, although this property was not mentioned there. Pastres et al.[34] modeled the water quality in a lagoon of Venice using a 1D reaction−diffusion model. The sensitivity curves of the phytoplankton concentration showed some global similarity. Mueller et al.[35] modeled the behavior of $H_2/O_2/NO_x$ and $CO/H_2O/O_2/NO_x$ reaction systems in a flow reactor, and several sensitivity profiles showed global similarity (see Figures 9, 10, and 18 in ref 35). Sensitivity curves, showing global similarity, appeared on the cover graphics of the book of Valkó and Vajda,[36] dealing with scientific computing methods. These sensitivity curves were calculated by an enzyme kinetic model.

Existences of local and global similarities of sensitivities are important features of mathematical models. Global similarity means that if several parameters are changed in a model, the effect can be fully compensated by changing a single effective parameter. This way the values of *all* variables can be restored to the original value in a *wide range* of time or distance. If local similarity is present, the values of *all* variables are restored simultaneously, but only at a point of the independent variable. In the case of empirical models, global similarity of sensitivities results in that very different parameter sets can produce exactly the same model results. If physical parameters are deduced by fitting to experimental data, error in the fixed parameters of a model having global similarity means that the determined values will be wrong even if the agreement between the data and the calculated values is excellent for all measured variables. Global similarity could be used to explain why the values of all variables in a wide spatial domain can be kept constant when several parameters are changing by regulating a single parameter only. This observation can be applied to the understanding of some self-regulating systems, like living organisms.

References and Notes

(1) Reuven, Y.; Smooke, M. D.; Rabitz, H. *J. Comput. Phys.* **1986**, *64*, 27.

(2) Smooke, M. D.; Rabitz, H.; Reuven, Y.; Dryer, F. L. *Combust. Sci. Technol.* **1988**, *59*, 295.

(3) Mishra, M. K.; Yetter, R.; Reuven, Y.; Rabitz, H. *Int. J. Chem. Kinet.* **1994**, *26*, 437.

(4) Rabitz, H.; Smooke, M. D. *J. Phys. Chem.* **1988**, *92*, 1110.

(5) Vajda, S.; Rabitz, H.; Yetter, R. A. *Combust. Flame* **1990**, *82*, 270.

(6) Vajda, S.; Rabitz, H. *Chem. Eng. Sci.* **1992**, *47*, 1063.

(7) Hughes, K. J.; Turányi, T.; Clague, A. R.; Pilling, M. J. *Int. J. Chem. Kinet.* **2001**, *33*, 513.

(8) *Combustion Simulations at the Leeds University and at the ELTE*; http://www.chem.leeds.ac.uk/Combustion/Combustion.html; http://garfield.chem.elte.hu/Combustion/Combustion.html.

(9) Kee, R. J.; Rupley, F. M.; Miller, J. A. *CHEMKIN−II: A FORTRAN chemical kinetics package for the analysis of gas-phase chemical kinetics*; SANDIA report No. SAND89-8009B; 1989.

(10) Lutz, A. E.; Kee, R. J.; Miller, J. A. *SENKIN: A FORTRAN program for predicting homogeneous gas-phase chemical kinetics with sensitivity analysis*; SANDIA report No. SAND87-8248; 1987.

(11) Kee, R. J.; Grcar, J. F.; Smooke, M. D.; Miller, J. A. *A Fortran program for modeling steady laminar one-dimensional premixed flames*; SANDIA report No. SAND85-8240; 1985.

(12) Glassmann, I. *Combustion*, 3rd ed.; Academic Press: San Diego, CA, 1996.

(13) Turányi, T. MECHMOD v. 1.4: Program for the transformation of kinetic mechanism available from ref 8.

(14) Saltelli, A., Scott, E. M., Chen, K., Eds. *Sensitivity analysis*; Wiley: Chichester, 2000.

(15) Turányi, T. *J. Math. Chem.* **1990**, *5*, 203.

(16) Tomlin, A. S.; Turányi, T.; Pilling, M. J. Mathematical tools for the construction, investigation and reduction of combustion mechanisms. In *Low-temperature combustion and autoignition*; Comprehensive chemical kinetics Vol. 35; Pilling, M. J., Ed.; Elsevier: Amsterdam, 1997; pp 293−437.

(17) Turányi, T.; Rabitz, H. Local methods. Chapter 9 (pp 81−99) in ref 14.

(18) Mishra, M.; Peiperl, L.; Reuven, Y.; Rabitz, H.; Yetter, R. A.; Smooke, M. D. *J. Phys. Chem.* **1991**, *95*, 3109.

(19) Rabitz, H. *Science* **1989**, *246*, 221.

(20) Bodenstein, M. *Z. Phys. Chem.* **1913**, *85*, 329.

(21) Turányi, T.; Tomlin, A. S.; Pilling, M. J. *J. Phys. Chem.* **1993**, *97*, 163.

(22) Lam, S. H.; Goussis, D. A. *Proc. Combust. Inst.* **1988**, *22*, 931.

(23) Lam, S. H. *Combust. Sci. Technol.* **1993**, *89*, 375.

(24) Lam, S. H.; Goussis, D. A. *Int. J. Chem. Kinet.* **1994**, *26*, 461.

(25) Roussel, M. R.; Fraser, S. J. *J. Chem. Phys.* **1991**, *94*, 7106.

(26) Maas, U.; Pope, S. B. *Combust. Flame* **1992**, *88*, 239.

(27) Maas, U.; Pope, S. B. *Proc. Combust. Inst.* **1994**, *25*, 1349.

(28) Maas, U. *Appl. Math.* **1995**, *40*, 249.

(29) Kaper, H. G.; Kaper, T. J. *Physica D* **2002**, *165*, 66.

(30) Eggels, R. L. G. M.; de Goey, L. P. H. *Combust. Flame* **1995**, *100*, 559.

(31) Büki, A.; Perger, T.; Turányi, T.; Maas, U. *J. Math. Chem.* **2002**, *31*, 345.

(32) Hughes, K. J.; Tomlin, A. S.; Hampartsoumian, E.; Nimmo, W.; Zsély, I. G.; Ujvári, M.; Turányi, T.; Clague, A. R.; Pilling, M. J. *Combust. Flame* **2001**, *124*, 573.

(33) Smith, J. M.; Szathmáry, E. *The origins of life. From the birth of life to the origin of language*; Oxford University Press: 1999.

(34) Pastres, R.; Franco, D.; Pecenik, G.; Solidoro, C.; Dejak, C. *Reliab. Eng. Syst. Safety* **1997**, *57*, 21.

(35) Mueller, M. A.; Yetter, R. A.; Dryer, F. L. *Int. J. Chem. Kinet.* **1999**, *31*, 705.

(36) Valkó, P.; Vajda, S. *Advanced scientific computing in Basic with applications in chemistry, biology and pharmacology*; Elsevier: Amsterdam, 1989.